GEOSPHERE

GEOSPHERE; v. 14, no. 6

https://doi.org/10.1130/GES01597.1

9 figures; 1 table

CORRESPONDENCE: enrico.cannao@unimi.it

CITATION: Cannaò, E., and Malaspina, N., 2018, From oceanic to continental subduction: Implications for the geochemical and redox evolution of the supra-subduction mantle: Geosphere, v. 14, no. 6, p. 2311–2336, https://doi.org/10.1130/GES01597.1.

Science Editor: Shanaka de Silva
Guest Associate Editor: Gray Bebout

Received 14 August 2017
Revision received 22 May 2018
Accepted 6 August 2018
Published online 2 October 2018

GOLD OPEN ACCESS

THE GEOLOGICAL SOCIETY OF AMERICA®

This paper is published under the terms of the CC-BY-NC license.

© 2018 The Authors

From oceanic to continental subduction: Implications for the geochemical and redox evolution of the supra-subduction mantle

E. Cannaò[1,2] and N. Malaspina[3]

[1]Dipartimento di Scienze della Terra "A. Desio," Università degli Studi di Milano, Via S. Botticelli 23, 20133 Milano, Italy
[2]Istituto di Geoscienze e Georisorse–CNR, Via Moruzzi 1, 56124 Pisa, Italy
[3]Dipartimento di Scienze dell'Ambiente e della Terra, Università degli Studi di Milano Bicocca, P.zza della Scienza 4, 20126 Milano, Italy

ABSTRACT

Processes taking place in subduction zones are the main controller of the chemical cycle of volatile and incompatible elements in the Earth system. Metamorphic devolatilization reactions occurring during slab burial play a key role in the transfer of elements to the supra-subduction mantle, from forearc to sub-arc depth. Here, we discuss the elements released in fluids and melts from oceanic (i.e., sediments, altered oceanic crust, and hydrated lithospheric mantle) and continental slab materials during prograde subduction and the consequent implications in the chemical evolution of the supra-subduction mantle. We use bulk data and fluid and melt inclusions analyses to show and to constrain the mobility of elements from top to bottom in the subduction zone setting. The development of mélange domains at the slab-mantle interface and its influence in the element cycle are also taken into account. Coupled with trace-element mobility, we review the redox evolution of slab materials during subduction and its implication in the redox conditions of the supra-subduction mantle due to fluid and melt infiltration down to sub-arc depth.

INTRODUCTION

Subduction processes are the main controller of the chemical cycle of volatile and incompatible elements in the Earth system (Stern, 2002; Elliott, 2004; Bebout, 2013; Schmidt and Poli, 2014; Hermann and Rubatto, 2014). The release of elements through dehydration and/or partial melting processes of the subducted materials is the main factor responsible for the metasomatism of the supra-subduction mantle. Generally, the subduction of oceanic lithosphere is promoted by its high density, thickness, and lower temperature with respect to the continental crust (e.g., Stern, 2002). However, the subduction of slices of continental crust up to ultra-high pressure (UHP) conditions is documented in several terranes by the discovery of UHP polymorphs such as coesite and diamond in gneisses or marbles (Chopin, 1984; Smith, 1984; Sobolev and Shatsky, 1990; Stöckhert et al., 2001). During the subduction path, slab rocks undergo chemical and physical transformations that are typical of high-pressure and low-temperature conditions, along a geotherm gradient from ~5–10 °C/km up to 20 °C/km (Peacock, 1996; Syracuse et al., 2010; Van Keken et al., 2011). Devolatilization reactions are the main processes promoting the slab-to-mantle element transfer and strongly depend on temperature. The temperature gradient of the subducting slab is consequently a key parameter controlling chemical evolution of the slab materials and the release of elements in the supra-subduction mantle (e.g., Van Keken et al., 2011). A full understanding of these transfer processes requires suitable rock samples that record interactions between mantle peridotites and incoming subduction fluids from forearc to sub-arc depths. Such samples correspond to metasomatized peridotites cropping out in orogenic environments, which are associated with crust-derived rocks both equilibrated at HP and UHP. Moreover, the investigation of the fluid phases produced by subducted oceanic lithosphere (i.e., by antigorite breakdown) and continental crust (i.e., aqueous fluids and supercritical liquids) and their interaction with the supra-subduction mantle enables us to unravel the possible metasomatic processes down to depths corresponding to arc magma sources.

The purpose of this contribution is to characterize the different geochemical fingerprints of the subducted oceanic lithosphere and continental crust through an overview of their trace-element signature and isotopic imprint. Also, we will consider the chemistry of fluid inclusions in both oceanic HP serpentinites and metasediments as representative of the composition of fluid phases able to metasomatize the supra-subduction mantle. To complete the picture, we will also present trace-element and isotopic data of supra-subduction peridotites affected by fluid phases derived from the continental crust at HP and UHP from three unique localities: Ulten Zone (Italian Central Alps), Sulu (Eastern China), and Bardane (Western Gneiss Region). All these results will be discussed in the framework of recent data available on the oxidizing capability of slab-derived fluid phases and of the oxidation state of the supra-subduction mantle at sub-arc depth.

In this contribution, we will try to address some important questions that are still under debate by the scientific community:

(1) How can the evolution of the subducting materials along the slab-mantle interface (from oceanic to continental crust) modify their geochemical features?

Downloaded from http://pubs.geoscienceworld.org/gsa/geosphere/article-pdf/14/6/2311/4578874/2311.pdf
by guest

(2) What is the role of subducted mineral assemblages as carriers of elements to depth?
(3) How can such evolution influence the geochemical features of the supra-subduction mantle?
(4) What is the redox state of the subducting lithosphere, and how does it evolve from oceanic to continental subduction?
(5) How can the redox-state evolution influence the speciation of elements in the metasomatic fluids infiltrating the supra-subduction mantle?

GEOCHEMISTRY OF SUBDUCTING MATERIALS

Subduction input materials are mainly constituted by the oceanic lithosphere, subdivided, from top to bottom, in oceanic sediments, altered oceanic crust, and hydrated lithospheric mantle. During the formation of an ocean by rifting processes, slices of continental crust from the margins may also occur as extensional allochthons in the newly formed basin (Peron-Pinvidic and Manatschal, 2010; Lundin and Doré, 2011; Beltrando et al., 2014). In this context, the subduction of the oceanic lithosphere can be associated with subduction of slices of continental crust (Dal Piaz, 1999; Mohn et al., 2014). Moreover, when the oceanic materials are consumed and entirely buried at depth, the subsequent continent-continent collision allows the subduction of portions of continental crust. In the following sections, the key points concerning the geochemistry of the oceanic lithosphere and continental crust, as "input subduction materials," are briefly described.

Oceanic Lithosphere

Sedimentary materials on the ocean floor represent the result of the erosion of continents and of biogeochemistry and marine life. The chemical composition of these materials can be considered as a mixing between multiple end-members of sediments that strongly depend on their source, such as continental and volcaniclastic detritus, biogenic carbonate and opal, Fe-Mn oxides, siliceous materials, and many others. As proposed by Plank and Langmuir (1998) and recently updated by Plank (2014), detrital components can provide alkali elements (K, Rb, and Cs), B, Be, Pb, and high field strength elements (HFSE: Hf, Zr, Nb, Ta, and Ti), whereas biogenic phases and biological productivity strongly affect the Ba and Sr contents. Lithium and rare-earth elements (REEs) are typical of the upper continental crust or average shales, while U seems mainly linked to organic C-rich sediments. Another key feature of sedimentary materials is their enrichment in some fluid-mobile elements, such as As and Sb (Li, 1991; Plank and Ludden, 1992). As will be discussed in the next sections, these elements play an important role in understanding the chemical exchange between different geochemical reservoirs during the subduction of oceanic lithosphere (Hattori and Guillot, 2007; Deschamps et al., 2011; Scambelluri et al., 2014; Cannaò et al., 2015; Scambelluri et al., 2015; Cannaò et al., 2016). From an isotopic point of view, the sedimentary material is characterized by strong enrichment in radiogenic isotopes, such as high $^{87}Sr/^{86}Sr$ ratios (0.7123 GLOSS II value) and Pb isotopes (e.g., Plank, 2014), due to the presence of micas that are the most important carrier of their parental elements Rb and Th-U, respectively. On the contrary, geochemical isotopic systematics of elements with high mantle affinity, such as Sm-Nd and Lu-Hf, are less radiogenic than mantle composition.

The oceanic crust forms at mid-ocean ridges by magmatism. Although quite homogeneous, its composition is related to the magma supply rates: In fast spreading ridges, magmas are generally more fractionated than those generated in slow spreading ridges (Perfit and Chadwick, 1998). Studies of the oceanic crust are accomplished through the collection of in situ drill cores, dredging of ocean floor, and by sampling and analyses of obducted ophiolitic sequences (e.g., Troodos in Cyprus and Samail in Oman). Based on major- and trace-element geochemistry analyses of these rocks, the average composition of the oceanic crust is typically mid-ocean ridge basalt (MORB), even if composition of MORB can vary substantially. The most important process able to strongly modify the elemental budget of the oceanic crust is the interaction with seawater or seawater-like fluids during hydrothermal alteration processes, contributing to the major addition of H_2O and CO_2 via crystallization of secondary hydrous- and carbon-bearing minerals (Staudigel, 2003, and references therein). In terms of trace elements, the formation of these alteration minerals allows the storage of elements derived from the seawater and the underlying sedimentary package. In this way, the oceanic crust may display positive anomalies in alkali elements, such as Cs, Rb, and K, and enrichment in B, Ba, Th, U, and S (Alt and Teagle, 2003). Also Li is a good indicator of hydrothermal interaction with seawater-derived fluids (Vils et al., 2008). Moreover, enrichment of some immobile elements such as REEs has been identified in extremely altered basalts dredged from some seamounts (Staudigel et al., 1996).

During the alteration process at the oceanic stage, the oceanic crust is affected by partial to complete resetting of its isotopic signature, which may diverge significantly from its original mantle value. Modification of stable (e.g., $\delta^{18}O$, δD, $\delta^{13}C$, $\delta^{11}B$, and $\delta^{37}Cl$) and radiogenic (e.g., $^{87}Sr/^{86}Sr$) isotopes may provide information about the oceanic alteration history of the crust. Subsequent subduction of these altered materials to mantle depth introduces significant geochemical anomalies with important consequence in the global element fluxes.

For the purpose of this review, we focus our attention on one of the most important isotopic systematics affected by alteration processes—the Sr ratio (Staudigel, 2003). Fresh crust shows the same Sr isotopic ratios of the depleted mantle ($^{87}Sr/^{86}Sr = 0.7025$; Klein, 2003), whereas the Sr signature of the altered oceanic crust will be close to that of the interacting fluids, which is much more radiogenic (e.g., present-day seawater $^{87}Sr/^{86}Sr = 0.7092$; Bruland et al., 2013). It is important to note that the Sr isotope ratio of seawater is affected by secular variation (McArthur et al., 2001). Due to the absence of isotopic fractionation during fluid production in subduction setting, the Sr isotopic signature of the fluids will be the same as that of the starting altered materials.

The lithospheric mantle is composed of depleted ultramafic rocks and therefore represents a poor geochemical reservoir (Niu, 2004). However, the

Downloaded from http://pubs.geoscienceworld.org/gsa/geosphere/article-pdf/14/6/2311/4578874/2311.pdf
by guest

hydration of the ocean floor strongly modifies the initial chemical composition of mantle rocks, and consequently, it changes their role in the *subduction factory* concept (Tatsumi, 2005). The hydration of mantle peridotites, i.e., serpentinization, is characterized by the development of serpentine minerals (plus minor amounts of brucite, chlorite, talc, tremolite, and magnetite), at the expense of olivine and pyroxenes. Serpentinites are mainly formed at slow to ultra-slow spreading ridges due to the exposure of the mantle on the seafloor by the occurrence of normal faults related to the extension and thinning of the crust along major scarps and transform faults (Bonatti, 1976; Morishita et al., 2009). These structures promote the infiltration of fluids enhancing the alteration of mantle rocks. More than ten years ago, Ranero et al. (2003) indicated that the presence of strike-normal faults near the trench, due to the bending of the subducting plate, promotes the deep hydration of the mantle with subsequent enrichment in some sediment-like elements, such as Cs, As, and Sb (Deschamps et al., 2011; Cannaò et al., 2016), with important implications in the subduction-related water cycle (Rüpke et al., 2004; Faccenda et al., 2009) and in the intermediate-depth seismicity (Ranero et al., 2005).

The presence of ~11%–15% of water into the crystal structure of serpentine minerals (e.g., chrysotile, lizardite, and antigorite) produces the most important chemical change in the oceanic lithospheric mantle prior to subduction. The geochemistry of serpentinites is quite homogeneous in terms of major elements, and the experimental study of Allen and Seyfried (2005) suggests that during seawater-peridotite interaction, the change in REE budget still reflects the geochemical imprint of the protolith. In this way, only the leftover trace-element contents will be affected by chemical depletion and/or enrichment, providing information about their geodynamic setting of formations (Deschamps et al., 2013). The entry of water in the crystal structure of serpentine minerals implies an increase of their molar volume, and therefore of the volume of the entire protolith (O'Hanley, 1992; Andreani et al., 2007), together with a decrease of density from 3.3 to 2.5 g/cm^3. This change of the mineral structure allows serpentine, in all its forms, to increase its trace-element budget (Mével, 2003; Niu, 2004; Scambelluri et al., 2004, 2014; Boschi et al., 2008; Vils et al., 2008; Deschamps et al., 2012; Kodolányi et al., 2012). As pointed out by Poli and Schmidt (2002), a peculiar, but relevant, lithology as CO_2 "input material" is represented by ophicarbonates. They consist of breccias of serpentinite clasts and micritic pelloids, cemented by a calcitic matrix, and often occur in ophiolite sequences (Schwarzenbach et al., 2013; Lafay et al., 2017). Despite their modest volume with respect to the rest of the oceanic lithosphere, they are able to transport high amounts of carbonates during subduction (Collins et al., 2015).

Hydration of the forearc mantle above the downgoing slab due to the uprising of slab-derived fluids may lead to the formation of supra-subduction serpentinites, such as in the Mariana forearc (Savov et al., 2007) or in now-exhumed mantle rocks (Hattori and Guillot, 2007). These serpentinites are characterized by enrichment in fluid-mobile elements, such as As, Sb, Cs, Pb, Th, U, and radiogenic Sr and Pb, with respect to the primitive mantle (PM) and abyssal serpentinites (Deschamps et al., 2012). In this respect, Peters et al. (2017) document that the use of U/alkali ratios may be a useful tool to unravel oceanic versus forearc origin of serpentinized mantle rocks. This approach is based on the redox-sensitive behavior of U in the two different geological settings coupled with the alkali-enriched source of the fluids hydrating the forearc region. The downward dragging of these materials at depth by subduction forces makes these rocks "a new" input material in subduction zones (Scambelluri and Tonarini, 2012). The original trace-element budget of the abyssal serpentinites can be modified by the interaction with slab fluids already at shallow depth, in correspondence with the lizardite to antigorite transition (e.g., Deschamps et al., 2011), as well as during a second event of serpentinization of partially oceanic serpentinized rocks (Hattori and Guillot, 2007; Cannaò et al., 2016). The typical sedimentary signature of these fluids allows serpentinites to increase their content of As and Sb, making these elements good candidates to track these processes (e.g., Hattori and Guillot, 2003).

As for the altered oceanic crust, the isotopic signature of the mantle rocks is reset due to hydration processes along the seafloor or in a forearc setting. In this way, the oceanic and forearc serpentinites will be characterized by different isotopic signatures (in particular for the $^{87}Sr/^{86}Sr$ ratio and Pb isotopes) that will be similar to those of the oceanic seawater for abyssal serpentinites or similar to those of the metamorphic fluids in the case of forearc and/or subducted serpentinites (e.g., Hattori and Guillot, 2007; Deschamps et al., 2012; Cannaò et al., 2016).

Continental Crust

Concerning the subduction of continental crust, Hermann and Rubatto (2014) highlighted that felsic crust, which typically consists of orthogneisses and paragneisses, is the predominant lithotype in UHP terrains, with a good affinity to the upper-middle continental crust (see Rudnick and Gao, 2014). The main mineral assemblage is represented by phengite + coesite + kyanite + garnet + clinopyroxene, where phengite is the most important carrier of large ion lithophile elements (LILEs), volatile and fluid-mobile elements, followed by clinopyroxene. Apatite, rutile, zircon, and allanite and/or monazite are the accessory phases that play an important role in the cycle of elements such as Ti, P, Th, and LREE (more than clinopyroxene, Hermann, 2002; Hermann and Rubatto, 2009). The presence of aqueous-rich fluids deriving from the destabilization of phengite or uprising from the subducting oceanic lithosphere at T > 650–700 °C, can trigger the wet partial melting of the subducted continental crust with very important implications on the slab-to-mantle mass transfer (Nichols et al., 1994; Schmidt et al., 2004; Auzanneau et al., 2006; Hermann et al., 2006; Hermann and Spandler, 2007; Hermann et al., 2013). Due to the high stability of phengite at dry conditions during deep subduction (Domanik and Holloway, 1996), the continental crust can provide large amounts of hydrous melt extremely enriched in LILE (Hermann et al., 2013; Zheng and Hermann, 2014). The capability of continental rocks to store H_2O is related to their composition in terms of MgO, K_2O, and CaO, which in turn controls the stabilization of talc, phengite, and epidote and/or amphibole, respectively (Hermann, 2002; Ferrando, 2012).

Downloaded from http://pubs.geoscienceworld.org/gsa/geosphere/article-pdf/14/6/2311/4578874/2311.pdf
by guest

The isotopic signature of the continental crust resembles that of the metasediments due to the high amount of minerals hosting Rb and Th-U, which decay during time in daughter ^{87}Sr and radiogenic Pb isotopes (^{206}Pb, ^{207}Pb, and ^{208}Pb), respectively.

SLAB FINGERPRINT PRESERVED IN FLUIDS RELEASED TO THE MANTLE

Fluids Produced by Oceanic Lithosphere versus Continental Crust: The Role of Phase Assemblages

To unravel the composition of the fluid phases released from the subducted oceanic lithosphere and continental crust to the supra-subduction mantle, we need to investigate their compositional evolution during subduction. The major- and trace-element concentration of slab-derived fluids strongly depends on their partitioning with stable assemblages. For this reason, in Figure 1, we report simplified phase diagrams for the different chemical constituents of the subducting slab (Fig. 1A: global subducted sediment [GLOSS]/continental crust; Fig. 1B: MORB + H_2O; Fig. 1C: peridotite + H_2O) and the elements released in the fluid phase after the complete breakdown of key hydrous minerals. The most representative reference works are reported in Table 1. Each pressure-temperature (P-T) diagram also reports the top-slab paths for hot and cold subduction zone (hot SZ and cold SZ, respectively) from Syracuse et al. (2010). The release of elements by mineral devolatilization in the following sections is described considering a static view of the subduction zone, with the hydrated lithospheric mantle at the bottom and the altered oceanic crust and metasediments lying above. Information about elements released from complex subduction setting, such as HP mélange, will be discussed in the next sections. Note that C-bearing phases are not considered in the following section, but we will treat their role in the redox evolution of the slab and supra-subduction mantle.

Metasediments

Metasediments are a complex and very heterogeneous lithology, and a global overview of the amount of elements transported to depth by subduction is difficult to obtain. The global subducted sediment (GLOSS and GLOSS II, Plank and Langmuir, 1998; Plank, 2014) may be considered as a proxy of the average starting materials of what are now the metamorphosed sedimentary rocks. At relatively low temperature (<200 °C) and below 1 GPa, the compaction of sediments enhances the release of elements hosted in the pore fluids (Fig. 1A; B, As, Sb, and Cs; Moore and Vrolijk, 1992), which are subsequently released during the evolution of subduction. The main minerals in the GLOSS/continental crust system able to release considerable amounts of elements during prograde to peak subduction are, in order of destabilization, amphibole, lawsonite, and phengite (and to a lesser extent biotite). Amphibole (glaucophane) breakdown occurs at ~500 °C, at very different pressures, from 1.0 GPa to 2.5 GPa, depending if in warm or cold subductions, respectively. The released fluid phase should be enriched in Be, B, and LILE (and possibly As and Sb and halogens; Bebout et al., 2007). The destabilization of lawsonite occurs at different P-T conditions: at high thermal conditions it is similar to those of amphibole, but in cold subductions lawsonite is stable up to 2.8 GPa at a temperature of ~600 °C (Fig. 1A; Martin et al., 2014). Similarly to amphibole, the main trace elements released by lawsonite destabilization are Be, B, LILE, U, Th, and Ce (and possibly As and Sb; Bebout et al., 2007). Phengite is the key phase able to provide high amounts of trace elements (LILE, LREE, B, and Li) during its breakdown. In wet conditions, phengite-out reaction occurs at ~650–700 °C and 2.0 or 3.0 GPa, in warm and cold subduction thermal settings, respectively (Fig. 1A). At dry conditions and in a closed system, phengite is stable down to UHP and ~1000 °C in warm subductions; whereas in cold subduction settings, it can reach depths compatible with pressures of 10 GPa (or even more), before melting (Domanik and Holloway, 1996).

Figure 2A reports the trace-element patterns of some prograde and HP metasediments from Catalina Schist (California, USA), Cima di Gagnone (Central Alps), and Schistes Lustrés (Western Alps), normalized to the GLOSS II. These terranes are representative of warm (Catalina Schist) versus cold (Alpine suite) subduction zone thermal settings at different peak conditions. In the Catalina Schist, Bebout and Barton (1993) and Bebout et al. (1999) document the loss of B, Be, As, Sb, Cs, and N during metamorphic devolatilization from lawsonite-albite and lawsonite-blueschist to epidote-amphibolite and amphibolite facies (see also Fig. 3). Due to the relatively warm subduction path followed by the Catalina Schist unit, the release of these elements occurs at T > 350 °C at ~1 GPa (Fig. 1A; Table 1). Examples of metasediments subducted at higher pressures along a cold subduction path are represented by paragneiss and micaschists from Cima di Gagnone (Central Alps), showing evidence of metamorphic peak conditions at ~2 GPa and 750 °C (Cannaò et al., 2015). These rocks are strongly depleted in fluid-mobile elements, such as Li, B, As, and Sb, and Zr-Hf, whereas they are enriched in Rb and K as well as LREE (and also U) due to the presence of stable white mica (mainly phengite) in the mineral assemblage. As shown in Figure 2A, compared to the Catalina Schist and the Cima di Gagnone metasediments, the Schistes Lustrés metasediments form the Western Alps do not display significant loss of elements from the sedimentary protoliths (Busigny et al., 2003; Chalot-Prat et al., 2003; Bebout et al., 2013). This could be due to the cold thermal regime of the fossil Alpine subduction zone with respect, for instance, to those of the Catalina Schist (e.g., Bebout et al., 2013). However, Lafay et al. (2013) and Cannaò et al. (2016) document depletion in some key fluid-mobile elements (As and Sb) in metasediments from the Queyras (Western Alps) and the Voltri Massif (Ligurian Western Alps), respectively (Fig. 3). Concerning this discrepancy, Busigny et al. (2003) proposed that the release of LILE and other incompatible elements may be controlled by the lithology of each sample, which, in turn, affects the devolatilization processes.

Downloaded from http://pubs.geoscienceworld.org/gsa/geosphere/article-pdf/14/6/2311/4578874/2311.pdf
by guest

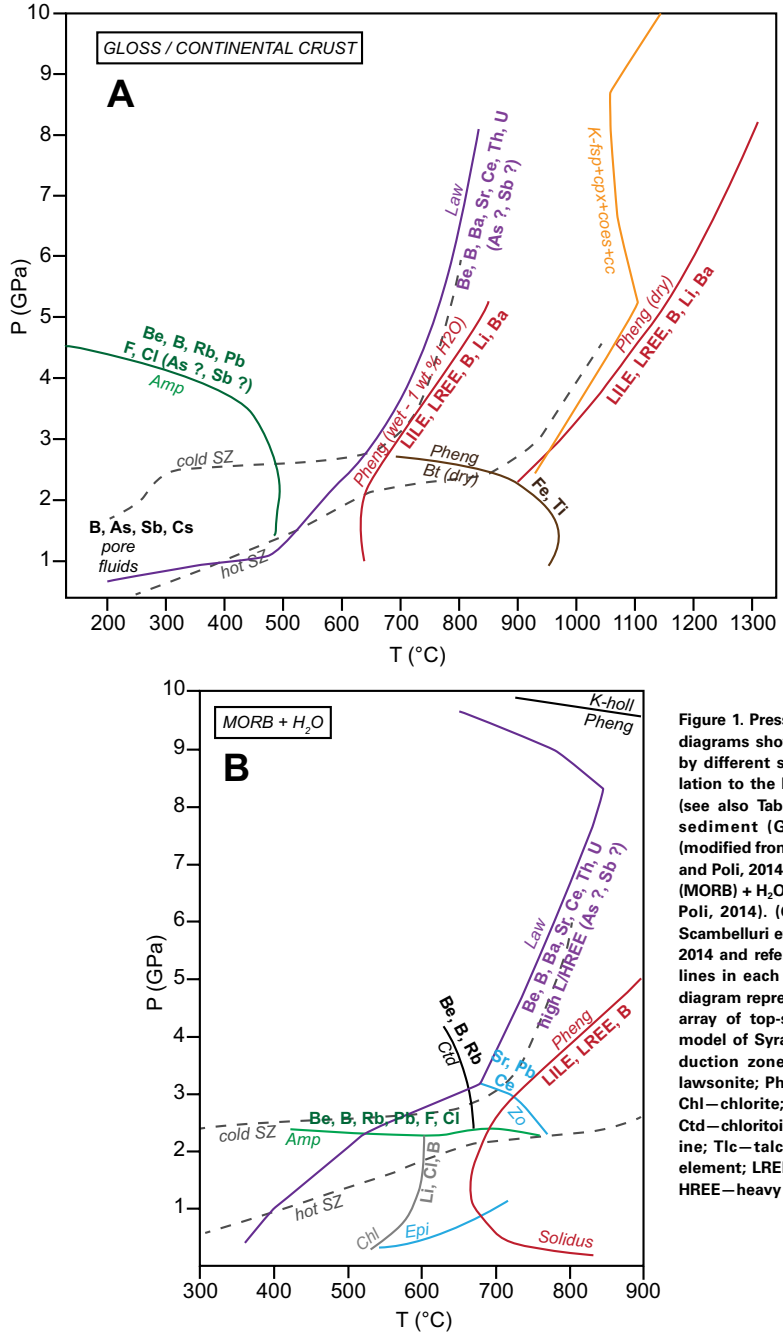

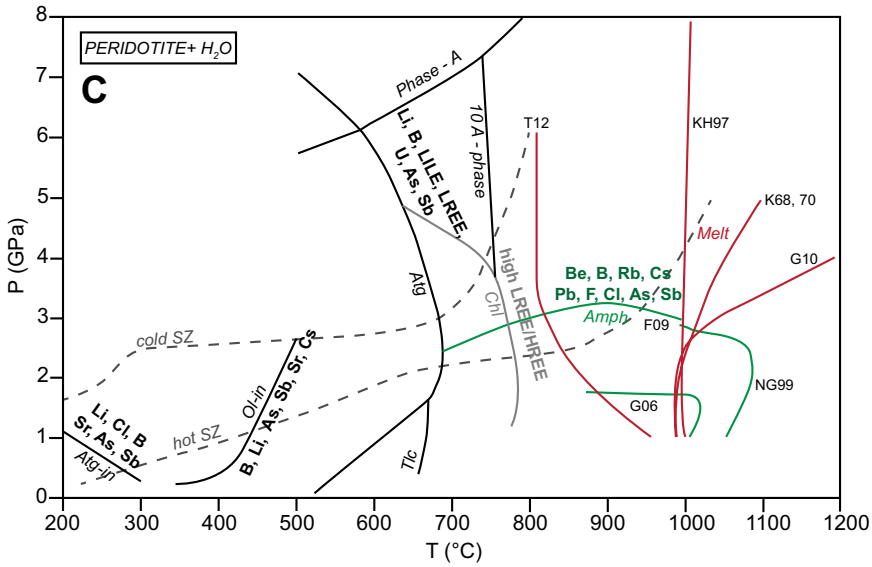

Figure 1. Pressure and temperature phase diagrams showing the released elements by different subducted lithologies in relation to the breakdown of major phases (see also Table 1). (A) Global subducted sediment (GLOSS)/continental crust (modified from Rüpke et al., 2004; Schmidt and Poli, 2014). (B) Mid-ocean ridge basalt (MORB) + H_2O (modifed from Schmidt and Poli, 2014). (C) Peridotites + H_2O (from Scambelluri et al., 1995; Schmidt and Poli, 2014 and references therein). Dotted gray lines in each pressure-temperature (P-T) diagram represent the range of the global array of top-slab geotherms of the D80 model of Syracuse et al. (2010). SZ—subduction zone; Amp—amphibole; Law—lawsonite; Pheng—phengite; Bt—biotite; Chl—chlorite; Epi—epidote; Zo—zoisite; Ctd—chloritoid; Atg—antigorite; Ol—olivine; Tlc—talc. LILE—large ion lithophile element; LREE—light rare-earth element; HREE—heavy rare-earth element.

Research Paper

Downloaded from http://pubs.geoscienceworld.org/gsa/geosphere/article-pdf/14/6/2311/4578874/2311.pdf
by guest

TABLE 1. TRACE ELMENTS RELEASED DURING PROGRADE SUBDUCTION BY THE DIFFERENT SUBDUCTED LITHOLOGIES

Lithology	Elements	Temperature (°C)	Pressure (Gpa)	References	Terranes
Marine sediments	B, As, Sb, Cs	<200	—	Moore and Vrolijk (1992)	Pore fluids
	B, Cs	200–300	0.9–1.2	Bebout et al. (1999)	Catalina Schist
	As, Sb	350–400	0.9–1.2	Bebout et al. (1999)	Catalina Schist
	Rb, Cs, B	300	<1.0	Sadofsky and Bebout (2003)	Franciscan Complex
	B, Li, Cs, Sr, As, Sb	350–400	0.9–1.5	Lafay et al. (2013)	Schistes Lustrés (Western Alps)
	B	350–450	2.0	Bebout et al. (2013)	Western Alps
	Sr, Li, B	300–400	0.9–1.2	Bebout et al. (2007)	Catalina Schist
	B, As, Sb, Pb, Sr	300–400	0.9–1.2	Cannaò et al. (2016)	Voltri Massif (Ligurian Alps)
	Li, B, Ba, As, Sb, Pb	300–400	0.9–1.2	Cannaò et al. (2015)	Cima di Gagnone (Central Alps)
Mafic oceanic crust	REE, Sr, Pb, U, Th	550–600	<1.6	Spandler et al. (2003)	New Caledonia
	Rb, Ba, Sr	<600	1.3–2.0	Arculus et al. (1999)	Raspas Complex (Ecuador)
	K, Rb, Ba, Pb	<600–700	1.3–1.5	Becker et al. (2000)	Different terranes
	Cs, Rb, Ba, K, B (?), High LREE/HREE, Sr	600–800	2.0–3.0	Vitale-Brovarone et al. (2014)	Alpine Corsica
	LILE, B,	700–800	4.0	Kessel et al. (2005a)	Experiment
	LILE, LREE, HFSE, Li, Be, B, Pb, Th, U	900–1000	4.0	Kessel et al. (2005a)	Experiment
	LILE, LREE, Li, Be, B, Nb, Ta, Pb, Th, U	800–900	6.0	Kessel et al. (2005a)	Experiment
	LILE, LREE, Li, Be, B, HFSE, Pb, Th, U	1000–1200	6.0	Kessel et al. (2005a)	Experiment
Oceanic lithospheric mantle	B, Li, Cl, Sr	550–600	2.0–2.5	Scambelluri et al. (2001, 2004)	Erro-Tobbio (Ligurian Alps)/ Almirez (Betic Cordillera)
	B, As, Sb, Cs, Sr, Pb	600–700	1.7–2.0	Peters et al. (2017)	Almirez (Betic Cordillera)
	Cs, Rb, Ba, U, Th, B, Pb, As, Sb, Li	700–800	2.3–3.0	Scambelluri et al. (2015)	Cima di Gagnone (Central Alps)
	Li, B, Sr, Cs, Ba, Pb, Th, U	700–900	3.5–4.0	Spandler et al. (2014)	Experiment
Continental crust	Cs, Rb, Pb, Sr	700–750	4.0–4.3	Ferrando et al. (2009)	Dora-Maira
	Rb, Ba, K, Pb, Th, U, Sr, LREE	1000	5.0	Stepanov et al. (2016)	Kokchetav Massif
	Cs, Rb, Ba, Pb, Th, U	600–650	2.2	Spandler et al. (2007)	Experiment
	LILE, LREE, Pb, Th, U	750–1050	2.5–4.5	Hermann and Rubatto (2009)	Experiment
	Cs, Rb, Ba, K, Th, U	750–1000	2.5–4.5	Zheng and Hermann (2014)	Experiment

Abbreviations: HFSE—high field strength element; LILE—large ion lithophile element; LREE—light rare-earth element; HREE—heavy rare-earth element; REE—rare-earth element.

Metabasalts

In a MORB + H_2O system (Fig. 1B; modified from Schmidt and Poli, 2014), the minerals able to transport at great depth significant amounts of trace and volatile elements are amphibole, lawsonite, phengite (in K-bearing system), together with chlorite, chloritoid, and epidote. As for the sedimentary system, the thermal setting of the subduction zone is crucial for the stability of lawsonite. In warm subduction zones, its breakdown reaction may occur at low temperature (400 °C) and pressure (1.0 GPa), whereas in cold subduction zones, its destabilization occurs at ~600 °C and 2.5 GPa (Fig. 1B; Schmidt and Poli, 1994). This is one of the most important reactions in a mafic system able to release considerable amounts of aqueous fluids enriched in incompatible elements (Be, B, Ba, U, Th, Ce, and Pb) and LREE at depth (e.g., Bebout et al., 2007; Vitale-Brovarone et al., 2014). Sodium-amphibole stability is P-dependent, occurring at ~2.0–2.5 GPa, for T ranging between 400 and 700 °C. Even if the amphibole/liquid partition coefficient for incompatible and LILE during amphibole formation in magmatic process is very low (Tiepolo et al., 2007), the formation of secondary amphibole on the ocean floor is associated with the incorporation of a relatively high amount of incompatible elements and halogens (e.g., Debret et al., 2016). The trace elements released in this reaction are similar to those for the sedimentary system (Figs. 1A and 1B). Also, Debret et al. (2016) document partial release of halogens and boron during prograde amphibole transformation from low-pressure polytype to glaucophane at ~1 GPa and 300–400 °C. Therefore, the real budget of element transfer to depth during complete amphibole dehydration may be influenced by these early stages of release.

At conditions of 550–600 °C and 1.0–2.5 GPa, chlorite destabilizes, releasing mainly Li, Cl, and B in the fluid phase (Fig. 1B). For Al-rich protoliths, at higher temperature and pressure conditions (600–650 °C; 2.5–4.0 GPa), the subduction

Downloaded from http://pubs.geoscienceworld.org/gsa/geosphere/article-pdf/14/6/2311/4578874/2311.pdf
by guest

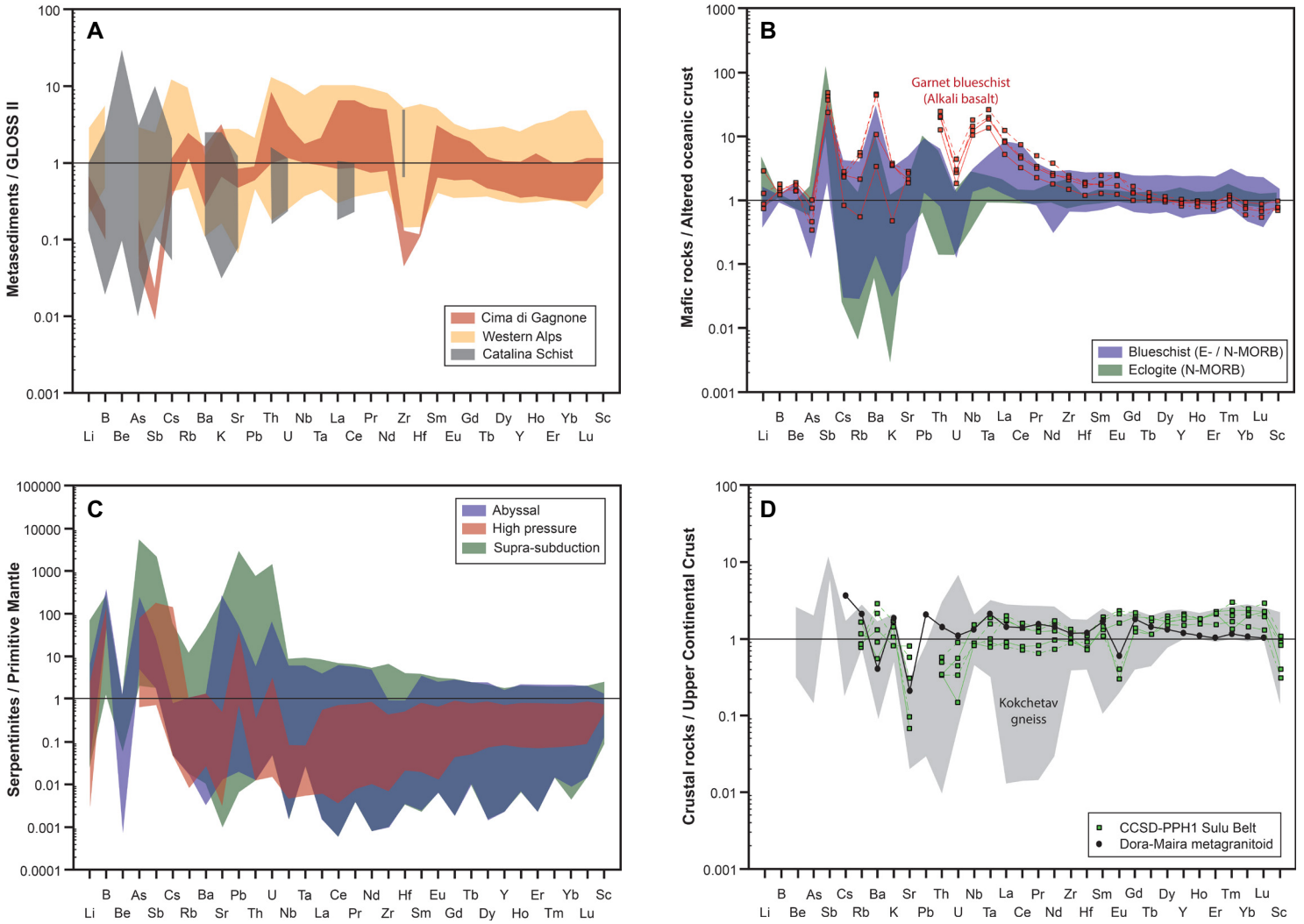

Figure 2. Trace-element composition of subduction input materials. (A) Metasediments normalized to global subducted sediment (GLOSS) II (Plank, 2014). Cima di Gagnone from Cannaò et al. (2015); Western Alps from Bebout et al. (2013) and Lafay et al. (2013); Catalina Schist from Bebout et al. (1999). (B) High-pressure mafic rocks normalized to altered oceanic crust (Onishi and Sandell, 1955; Smith et al., 1995; Kelley et al., 2003). Blueschist and eclogite rocks from Becker et al. (2000), Spandler et al. (2004), and John et al. (2010). (C) Abyssal, subducted, and supra-subduction serpentinites normalized to primitive mantle (McDonough and Sun, 1995). Abyssal serpentinite from Paulick et al. (2006) and Kodolányi et al. (2012); subducted serpentinites from Lafay et al. (2013), Debret et al. (2013), and Cannaò et al. (2016); supra-subduction serpentinites from Ishii et al. (1992), Lagabrielle et al. (1992), Parkinson and Pearce (1998), Pearce et al. (2000, 2005), Guillot et al. (2001), Savov et al. (2005, 2007), Hattori and Guillot (2003, 2007), Marchesi et al. (2006, 2009), Saumur et al. (2010), Deschamps et al. (2012), Blanco-Quintero et al. (2011), and Kodolányi et al. (2012). (D) Continental crust normalized to upper continental crust (Rudnick and Gao, 2014). Dora-Maira from Ferrando et al. (2009); Kokchetav gneiss from Stepanov et al. (2014); Chinese Continental Scientific Drilling Pre-Pilot Hole 1 (CCSD-PPH1) of the Sulu Belt from Zhang et al. (2005).

Downloaded from http://pubs.geoscienceworld.org/gsa/geosphere/article-pdf/14/6/2311/4578874/2311.pdf
by guest

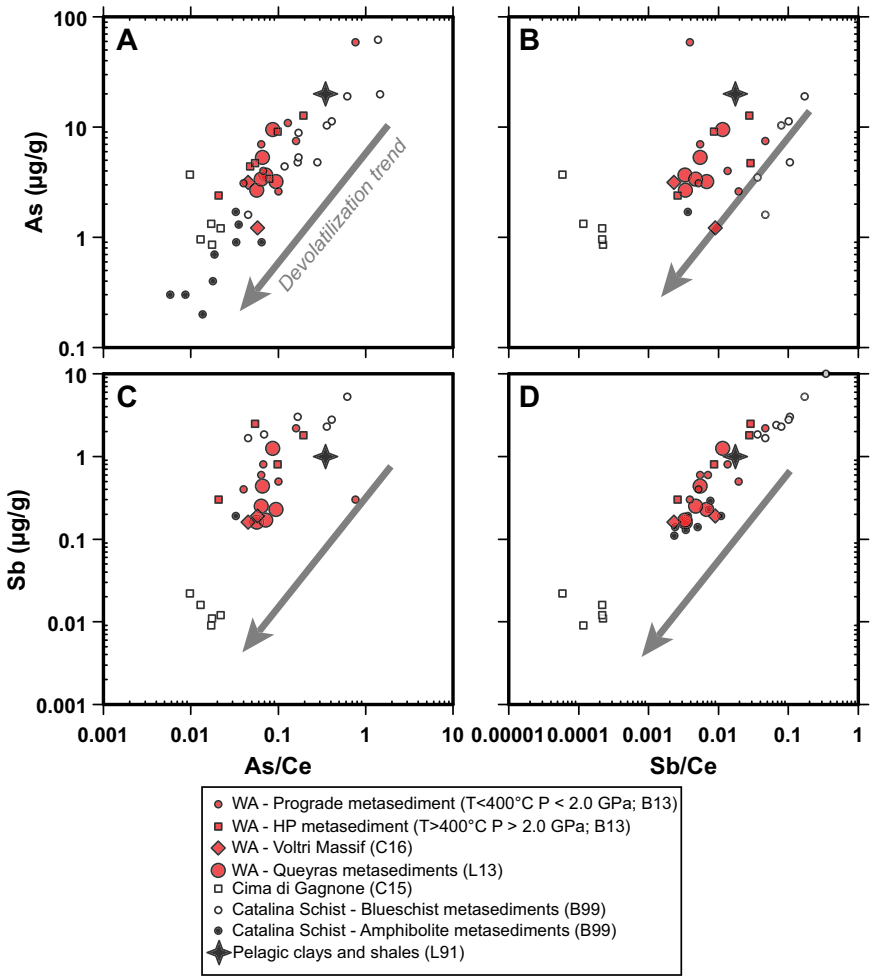

Figure 3. (A–D) As and Sb versus As/Ce and Sb/Ce diagrams for metasedimentary rocks from Western Alps (WA; B13: Bebout et al., 2013; L13: Lafay et al., 2013; C16: Cannaò et al., 2016), Catalina Schist (B99: Bebout et al., 1999) and Cima di Gagnone (C15: Cannaò et al., 2015), compared with pelagic clays and shales (L91: Li, 1991). The gray arrow shows the devolatilization trend due to As and Sb loss during early prograde subduction processes.

path reaches the breakdown of chloritoid, which is able to release trace elements such as Be, B, and Rb (Xiao et al., 2016). At similar pressures but at T = 650–750 °C, epidote (zoisite) breakdown provides significant amounts of Sr, Pb, and Ce (and light rare-earth elements [LREEs]; e.g., Xiao et al., 2016). Recent experimental studies by Carter et al. (2015) propose that Fe^{3+}-bearing epidote may be stable at higher temperature (up to 900 °C) at 3 GPa, controlling the release of LREE and Th to the fluid phase. The destabilization of phengite corresponds to the partial melting condition of mafic systems at water-saturated conditions and occurs at relatively HT-HP (>700 °C and >2 GPa). During this process, phengite transfers large quantities of trace elements in the melt phase (LILE, LREE, and B). Similarly to what happens in the metasedimentary system, minor accessory phases are able to play an important role in the partitioning of Ti, Nb, Ta (rutile), LREE, Th, Sr, Pb (allanite), P, LREE, Th, U (apatite), and Zr, Hf (zircon) (Hermann, 2002; Zack et al., 2002; Rubatto and Hermann, 2003; Spandler et al., 2003; Klimm et al., 2008). Recently, Tsay et al. (2017) proposed that the addition of various ligands into the fluid phase, such as Cl and F, might affect the solubility of elements thus controlling their partitioning and mobility.

Figure 2B portrays the trace-element composition of blueschist- and eclogite-facies mafic rocks from several metamorphic terranes (Raspas Complex, Western Alps, and New Caledonia; data from Becker et al., 2000; Spandler et al.,

Downloaded from http://pubs.geoscienceworld.org/gsa/geosphere/article-pdf/14/6/2311/4578874/2311.pdf
by guest

2004; John et al., 2010) normalized to the altered oceanic crust (AOC; Smith et al., 1995; Onishi and Sandell, 1955; Kelley et al., 2003). It must be specified that the composition of AOC could be extremely variable, depending on the alteration degree of the original protolith. In order to better unravel the potential trace-element release from subducted oceanic mafic crust affected by the major dehydration process within the downgoing slab (the blueschist-eclogite transition; Peacock, 1993), in Figure 2B, we consider rocks showing affinity with the enriched and normal MORB (enriched [E]- and normal [N]-MORB, respectively), as well as alkali basalt. Blueschist mafic rocks display a relatively narrow pattern of element concentration variability for Li, B, Be, and As together with the REE. The concentration of these elements is close to 1 × AOC up to 10 × AOC values. The most incompatible and fluid-mobile elements show a wide range of concentrations, with Cs, Rb, K, and U characterized by negative anomalies, and Sb, Ba, Pb, and Th showing an opposite behavior. Mafic rocks re-equilibrated under eclogite-facies conditions show similar trace-element patterns even if they are characterized by the depletion in almost all elements (except Sb, Pb, and Th). Garnet-bearing blueschist mafic rocks showing affinity with alkali basalt are strongly enriched in LREE and LILE reflecting the high modal amount of phengite and amphibole in the mineral assemblages. This lithology is expected to introduce high amounts of incompatible elements into depth during phengite and amphibole destabilization.

In contrast to this evidence, Spandler et al. (2003) document insignificant element mobility during prograde metamorphism from lawsonite-blueschist to eclogite facies in HP metabasalts from New Caledonia. These authors provide evidence that the trace elements released during blueschist mineral breakdown reactions are retained in the newly formed major and accessory minerals, such as epidote, phengite, garnet, rutile, and zircon. This implies that eclogitic minerals still retain significant amounts of elements leading to the release of huge quantities of aqueous fluids depleted in trace elements (Spandler et al., 2003).

Serpentinites

In the hydrous peridotite system (Fig. 1C), serpentine is the most important mineral capable of trapping, transporting, and releasing volatiles and key trace elements at great depth (Ulmer and Trommsdorff, 1995; Scambelluri and Philippot, 2001; Scambelluri et al., 2001, 2004, 2007, 2014, 2015). The phase transition from lizardite and/or chrysotile to antigorite at T <300 °C and low P, is associated with the partial release of Li, Cl, B, Sr, As, and Sb from the system, due to changes in the mineral structure and the loss of ~2 wt% of water (Kodolányi and Pettke, 2011). During the olivine-in reaction (400–500 °C; 0.5–2.5 GPa), these elements are lost (Deschamps et al., 2011; Lafay et al., 2013) even if metamorphic olivine is still able to retain a significant amount of them (e.g., B, As, and Sb, Tenthorey and Hermann, 2004; Scambelluri et al., 2014). The complete breakdown of antigorite is mainly temperature dependent (Ulmer and Trommsdorff, 1995; Wunder and Schreyer, 1997) and occurs at T between 600 and 700 °C, in relation to its Al content (Padrón-Navarta et al., 2013). Due to the "sponge-like" behavior characterizing serpentine (e.g., Deschamps et al., 2011; Lafay et al., 2013; Cannaò et al., 2015, 2016), the fluid-mediated mass transfer processes, occurring during prograde subduction in a top slab mélange setting, as well as in peridotites from a supra-subduction setting, allow serpentinites to be enriched in exogenous elements (LILE, LREE, and fluid-mobile element). All these elements will then be released upon complete antigorite destabilization.

In addition to serpentine, chlorite and amphibole are also able to release some trace elements after their breakdown. Chlorite destabilization occurs at higher temperature (700–800 °C) and in the presence of garnet may provide high LREEs and heavy rare-earth elements (HREEs) in the fluid phase coupled with Cl and Li. Calcic amphibole can be present in the HP mineral assemblage of subducted-derived metaperidotite (i.e., the product of complete dehydration of serpentinite precursor; Scambelluri et al., 2014) and represents the last hydrous phase enriched in incompatible elements, able to release B, As, Sb, LILE, and Pb (and potentially halogens). As for the other systems, its stability is mainly P-dependent (2.5–3.0 GPa) at T up to 900–1000 °C (Fumagalli and Poli, 2005). Among accessory phases, the most important ultramafic systems are the humite-type minerals (clinohumite, humite, chondrodite, and norbergite). It is indeed well known that the stability of clinohumite increases with the increase of its F/OH ratio, acting as carrier of volatiles and halogens into the deeper parts of the mantle (Engi and Lindsley, 1980; Trommsdorff and Evans, 1980; Evans and Trommsdorff, 1983; Weiss, 1997; Stalder and Ulmer, 2001; López Sánchez-Vizcaíno et al., 2005; Hermann et al., 2007; John et al., 2011). The new experimental data by Grützner et al. (2017) suggest that F-bearing humites could be stable even at conditions corresponding to the transition zone (up to 1800 °C at 17 GPa).

In Figure 2C, the primitive mantle (PM) normalized (McDonough and Sun, 1995) trace-element patterns of subducted HP serpentinites and from supra-subduction settings are compared with those of abyssal serpentinites. Abyssal serpentinites, before subduction, may be enriched in halogens (not shown in the plot; Kendrick et al., 2011, 2013, 2017; John et al., 2011) and B, As, Sb, Sr, U, and Li (Paulick et al., 2006; Delacour et al., 2008; Vils et al., 2008; Kodolányi and Pettke, 2011; Augustin et al., 2012). Boron and As are the only elements always above the PM values, whereas Be shows a negative anomaly and is always below the PM value as well as other LILEs (Cs, Rb, and Ba). During subduction, serpentinites maintain the trace-element budget acquired from oceanic serpentinization (cf. purple and yellow patterns of Fig. 2C) and thus are even more enriched in As, Sb, and Cs. Also supra-subduction serpentinites record enrichment in these elements, reaching absolute values of As, Sb, Pb, Th, and U > 1000 × PM. The previously mentioned characteristics are likely acquired during the fluid-mediated mass transfer at the slab-mantle interface, between serpentinites and the other slab reservoirs (altered oceanic crust and/or sediments). This exchange allows HP and supra-subduction serpentinites to acquire hybrid and unusual geochemical signature also in terms of B, Sr, and Pb isotopic compositions (e.g., Deschamps et al., 2011, 2012; Lafay et al., 2013; Cannaò et al., 2015, 2016). Evidence of these interactions is well recorded in several Alpine mélange-type terranes and seems to have occurred during their prograde subduction (Lafay et al., 2013; Cannaò et al., 2015, 2016).

Downloaded from http://pubs.geoscienceworld.org/gsa/geosphere/article-pdf/14/6/2311/4578874/2311.pdf
by guest

Continental Crust

The main difference between the oceanic lithosphere and the continental crust in terms of dehydration during prograde subduction is that sediments and altered oceanic crustal rocks progressively lose H_2O during their burial, due to water-conservative metamorphic reactions taking place within the slab (e.g., Schmidt and Poli, 2014). At the same time, beyond the antigorite and chlorite breakdown (and phase-A at low T), H_2O can be stored only in continental crust lithologies (in phengite, talc, and amphibole). In particular, Hermann (2002) suggested that the hydration of dry continental crust by metamorphic slab fluids is able to stabilize phengite at the expense of K-feldspar, as documented, for example, in the Dora-Maira Massif (Biino and Compagnoni, 1992; Compagnoni et al., 1995; Ferrando et al., 2009). Similarly, chloritization of granitic rocks and formation of talc and phlogopite in Mg-rich system are processes that provide a significant amount of water even in continental rocks at H_2O-undersaturated conditions (Schertl and Schreyer, 2008). In this way, the continental crust may also become an important reservoir for H_2O. Subduction of portions of continental crust is able to reach UHP conditions in a cold subduction thermal setting prior to phengite-dehydration melting. In this way, deep element transfer from continental crust allows the release of a high amount of LILE and incompatible elements to the supra-subduction region.

The most famous terranes where exhumation of UHP continental crust occurs are the Kokchetav Massif (Northern Kazakhstan), Dora-Maira (Western Alps), and Sulu Belt (Eastern China). As shown in Figure 2D, the gneiss from Kokchetav (Stepanov et al., 2014) normalized to the upper continental crust (UCC, Rudnick and Gao, 2014) displays quite uniform middle–heavy rare-earth element (M-HREE) patterns ranging from 1 to 3 times the UCC values (except for Sm with a slight negative anomalies). On the other hand, the compositional range of the LREE is much more widespread, with a strong negative anomaly down to two orders of magnitude with respect to the UCC. This high variability in the LREE budget is related to the amount of white mica present in the gneisses coupled with the complete dissolution of monazite and allanite during melt production in the most restitic portion of the rocks (Stepanov et al., 2014). Strontium, Pb, and Th show a similar trend to that of the LREE, whereas U may reach up to 10 times the UCC value. The LILE pattern is scattered, with negative anomalies in Cs and Ba and positive anomalies for Rb and K. Antimony is always positive up to one order of magnitude higher than the UCC value, whereas As and Be range from 2 to 0.2 times the UCC values (Fig. 2D). No data about Li and B are available in the literature. The metagranite from Dora-Maira (Ferrando et al., 2009) normalized to the UCC shows relative depletion in M- and HREE and almost flat LREE pattern with a negative Eu anomaly (Fig. 2D), with concentrations always above those of the UCC. Lead and Th are slightly enriched, and U is close to the UCC value. Barium and Sr display negative anomalies, whereas other LILEs appear enriched. Continental crustal rocks from the Sulu Belt display almost flat REE patterns, with no significant depletion in LREE in some samples. A negative Eu anomaly is present for a couple of samples. Uranium, Th, and Sr show a relatively wide range of variation and values always below the UCC, whereas the other LILE are mostly above UCC. No data for Li, B, Be, As, and Sb from these two massifs are currently available in literature.

Overall, it seems that the gneiss from Kokchetav massif is much more depleted in LREE. This is probably due to the partial melting that occurred during their subduction and exhumation history, as testified by the presence of multiple melt inclusions in garnet (Stepanov et al., 2014, 2016). Nevertheless, their LILE concentrations are still comparable with those of the UCC. Compared to the Kokchetav Massif, the gneiss and metagranite from Sulu and Dora-Maira do not show evidence of partial melting consistent with the relative enrichment in LILE characterized by the occurrence of stable phengite in these rocks.

Slab-Derived Fluid Composition: Evidence from Fluid/Melt Inclusions

The occurrence of fluid/melt or multiphase solid inclusions in the newly formed metamorphic anhydrous minerals, such as garnet or omphacite in eclogites and olivine and enstatite in serpentinites, witnesses the entrapment of fluid or melt phases (or supercritical liquids above the second critical endpoint) produced by the dehydration reactions previously described. A P-T compilation of HP and UHP terranes where fluid/melt inclusions have been characterized is displayed in Figure 4. The laser ablation analyses of these inclusions allow the determination of their compositions in terms of trace elements. In Figure 5, we report natural and experimental trace-element data of aqueous fluids, supercritical liquids, and melt inclusions occurring in eclogite-facies rocks representing the different input subduction zone components, normalized to the PM values (Fig. 5A: continental crust and/or sediments; Fig. 5B: oceanic crust; Fig. 5C: ultramafic rocks).

Multiphase solid inclusions from Dora-Maira whiteschist (Ferrando et al., 2009) and melt inclusions from gneisses of the Kokchetav massif (Stepanov et al., 2016) may be considered as proxies of the compositional evolution recorded by fluids in metasediments during their subduction to UHP, with enrichment in the most incompatible trace elements. The fluid inclusions within the garnet in the whiteschist from the Dora-Maira UHP unit are representative of the fluid released during the peak condition via the reactions: phlogopite + kyanite + talc = garnet + phengite + fluid and kyanite + talc = garnet + coesite + fluid (Ferrando et al., 2009). This fluid is strongly enriched in LILE and U, relatively enriched in Ba and Th, and is depleted in HFSE. Inclusions hosted in garnet from the Kokchetav UHP gneiss represent the product of partial melting at 4.5 GPa and ~1000 °C. During this process, LILE, LREE, Th, and U are released in the melt phase. As shown in Figure 5A, these different inclusions show visible differences in their LILE and LREE concentrations, as well as in U and Th. These are related to the presence of stable phengite in the mineral assemblage of the Dora-Maira rocks, which partitions most of the LILE. Melt inclusions from the Kokchetav rocks derive from the partial melting induced by the destabilization of phengite. For comparison, in Figure 5A, we also reported the composition of experimental aqueous fluids and hydrous melts (Spandler et al., 2007; Hermann and Rubatto, 2009; Zheng and Hermann, 2014). These are similar to natural fluid/melt inclusions in terms of element mobility, showing

Downloaded from http://pubs.geoscienceworld.org/gsa/geosphere/article-pdf/14/6/2311/4578874/2311.pdf
by guest

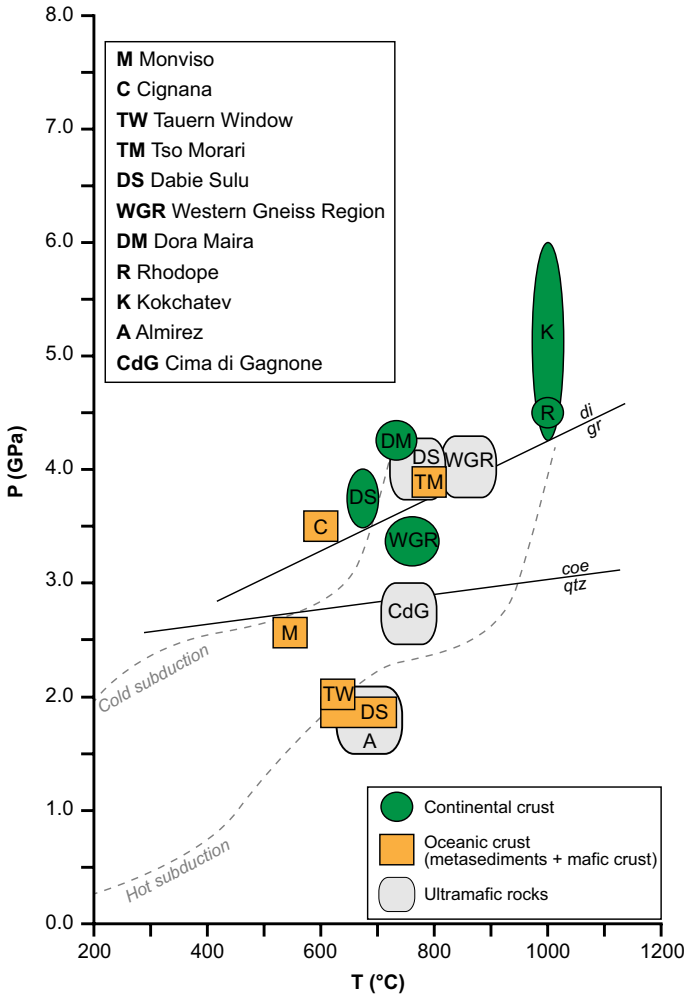

Figure 4. Pressure-temperature (P-T) conditions of high-pressure and ultrahigh-pressure complex subdivided in oceanic crust (metasediments + eclogite, orange areas), ultramafic rocks (gray areas), and continental crust (green areas) based on fluid/melt inclusions occurrence (modified from Frezzotti and Ferrando, 2015).

enrichment in LILE, Pb, Th, and U. The main difference is that these elements are much more concentrated in the hydrous melt than in the aqueous fluids, in agreement with the ability of hydrous melts to mobilize trace elements as discussed by Hermann et al. (2006). Again, it should be noted that no data about Li, Be, and Sb concentrations in fluid/melt inclusions in sediment/continental crust occur in the literature as of now.

Concerning the oceanic crust (Fig. 5B), the multiphase solid inclusions hosted in garnet of the UHP eclogite from Sulu (China; Gao et al., 2012, 2013) show enrichment in Rb, Ba, K, and Sr coupled with variable enrichment in Pb, Th, and U, depletion in HFSE and more enrichment in LILE than LREE. These inclusions are interpreted to be the product of the dehydration melting of eclogite during phengite breakdown. The trace-element signatures of K-free MORB-derived supercritical liquids and melts were determined experimentally for T ranging between 700 and 1200 °C and P = 4–6 GPa by (Kessel et al., 2005a, 2005b). Both supercritical liquids (LT) and melts (HT) are enriched in B, Li, LILE, and LREE. The supercritical liquids at 6 GPa show a relatively narrow range of trace-element concentrations in relation to the temperature variation. Conversely, in the supercritical liquids at lower pressure (4 GPa), the trace-element concentrations are much more temperature dependent, suggesting an increase of the fluid/solid partition coefficient with increasing temperature for the analyzed elements. Recently, Carter et al. (2015) experimentally documented the element release by MORB and AOC system (K_2O wt% is the main difference) at 3 GPa and T ranging from 750 to 1000 °C. Their results show several discrepancies compared to previous studies, in particular due to abundant residual epidote storing Th and LREE. The increase of the LILE content in the melt with temperature is always related to the partial destabilization of phengite. Other experimental studies focused on understanding the mobility and fractionation of REE in aqueous fluids during the slab dehydration at 2.6 GPa and T from 600 to 800 °C, were carried out by Tsay et al. (2014; not shown in figure 5B). These authors document the increase in the REE contents of the aqueous fluid with the increase of temperature, also promoted by the presence of additional ligands such as Cl^-, F^-, CO_3^{2-} and SO_4^{2-}. A different behavior is recorded by HREE and HFSE. Crystallization of garnet and accessory minerals, such as zircon and rutile, during the opening of HP veins in eclogites promotes the partitioning of HREE and HFSE, respectively. Such a partitioning leads to low mobility of these elements in the fluid phase during the dehydration of the oceanic crust (Rubatto and Hermann, 2003). To date, no data about fluid mobile As and Sb are documented in literature.

Figure 5C shows the composition of multiphase solid and aqueous fluid inclusions hosted by olivine and garnet in metaperidotites from Cerro del Almirez (Betic Cordillera) and Cima di Gagnone (CdG, Central Alps) HP and UHP ultramafic rocks. They represent the product of partial (Almirez) to complete (CdG) dehydration of serpentinites and serpentinized peridotites (Evans and Tromsdorff, 1978; Scambelluri et al., 2014). These data are compared with the experimental study performed by Spandler et al. (2014). The fluid inclusions hosted in metamorphic olivine are believed to represent the fluid composition produced by the antigorite breakdown, whereas the fluid inclusions hosted in garnet represent the remnants of the fluids released after the chlorite-out reaction (see also Fig. 1C; Scambelluri et al., 2015). The full trace-element composition of fluid inclusions from Almirez is reported in Peters et al. (2017, and references therein) showing enrichment in Li, B, As, Sb, Pb, Th, and LILE and LREE are close to 1 × PM. Multiphase solid inclusions hosted in the metamorphic olivine of the chlorite harzburgite from CdG show comparable

Downloaded from http://pubs.geoscienceworld.org/gsa/geosphere/article-pdf/14/6/2311/4578874/2311.pdf
by guest

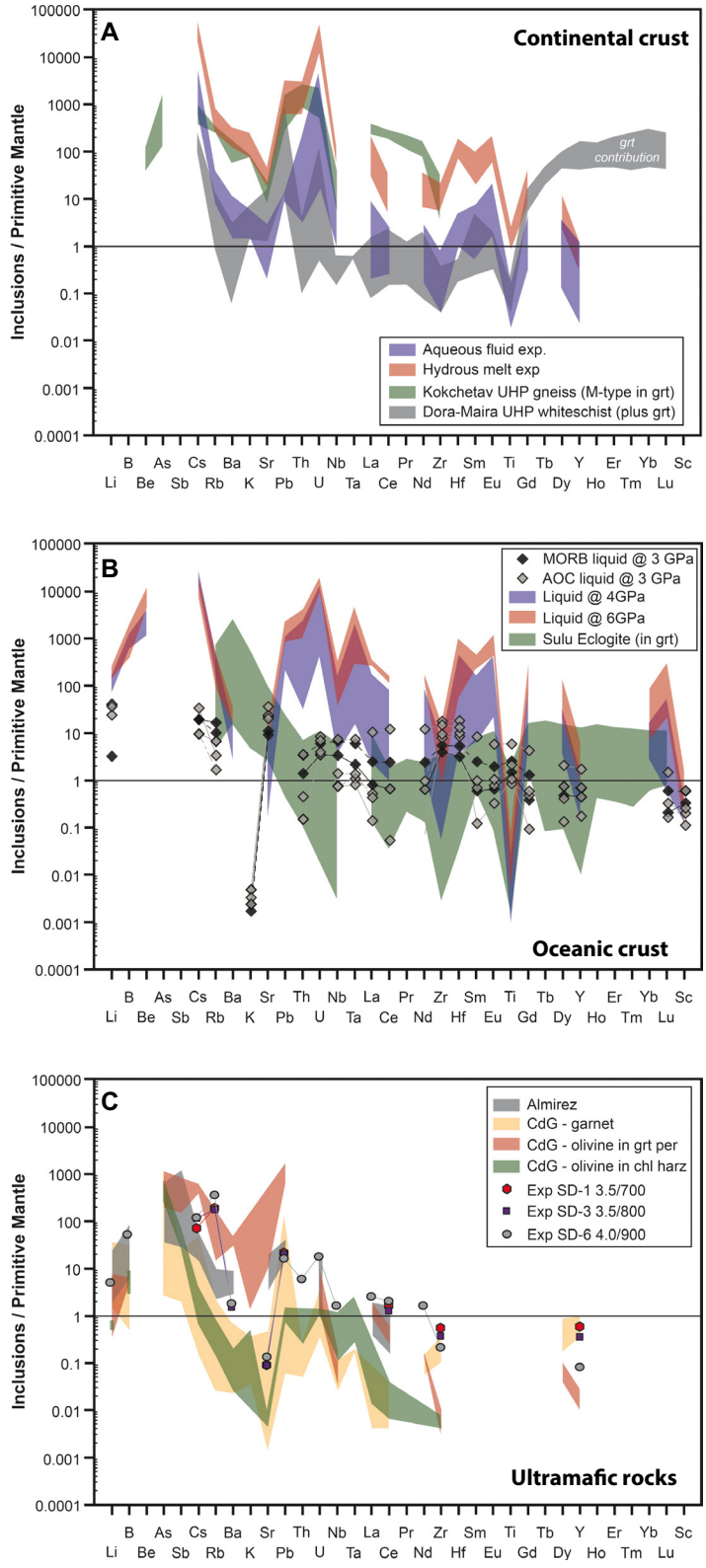

Figure 5. Trace-element patterns of natural and experimental fluid/melt inclusions normalized to primitive mantle (McDonough and Sun, 1995) for (A) continental crust (Dora-Maira: Ferrando et al., 2009; Kokchetav: Stepanov et al., 2016); aqueous fluid experiment (Spandler et al., 2007, and Zheng and Hermann, 2014); hydrous melt experiment (Hermann and Rubatto, 2009); (B) oceanic crust (eclogite in Sulu terrane: Gao et al., 2013); liquid experiment (Kessel et al., 2005a); mid-ocean ridge basalt (MORB) and altered oceanic crust (AOC) experiment (Carter et al., 2015); and (C) ultramafic rocks (Cima di Gagnone [CdG]: Scambelluri et al., 2015; Almirez: Peters et al., 2017); experimental results (Exp SD) from Spandler et al. (2014) at different pressure (3.5–4.0 GPa) and temperature (700 – 900 °C) conditions. UHP—ultrahigh-pressure.

Downloaded from http://pubs.geoscienceworld.org/gsa/geosphere/article-pdf/14/6/2311/4578874/2311.pdf
by guest

enrichment in B but, overall, a decrease in all other trace elements such as LILE down to 1 × PM or even below. On the contrary, the same inclusions hosted in olivine form the garnet peridotites display strong enrichments in As, Sb, and LILE. The trace-element budget of the fluid produced by the chlorite dehydration at higher temperature is represented by the yellow field in Figure 5C. This fluid is less enriched in incompatible elements with respect to those of the olivine inclusions but still preserves B, As, and Sb contents higher than those of the PM. It is interesting to note that previous trace-element and isotopic studies on these localities provided the evidence that Almirez and Cima di Gagnone ultramafic rocks were affected by a different grade of interaction with sediment-derived fluids during prograde subduction (Marchesi et al., 2013; Harvey et al., 2014; Cannaò et al., 2015). This process may explain the enrichment in incompatible and fluid-mobile elements shown by these fluids. Here, we want to highlight that, to date, the pure geochemical signatures of abyssal serpentinite component transported at depth are still missing due to the sponge-like behavior of serpentinized mantle rocks during subduction processes (e.g., Deschamps et al., 2011; Cannaò et al., 2016).

From an experimental point of view, Spandler et al. (2014) showed that the trace elements released during UHP serpentinite dehydration at 3.5 GPa and 700–800 °C consist of Li, B, LILE, LREE, and U in the fluid phase. Chlorite dehydration, at higher P-T conditions (4.0 GPa and 900 °C), produces fluids with high LREE and HREE and Ce/Y ratios, due to retention of HREE and Y in the newly formed garnet.

REDOX EVOLUTION DURING SUBDUCTION

When we consider geochemical fluxes at subduction zones, we must pay attention to elements that are sensitive to the redox conditions of the system (e.g., Fe, C, S, Mn, P, and U). These elements occur in different oxidation states and in variable concentrations within the slab lithologies and may be released after a change in their oxidation state during subduction (Evans, 2012). As an example, carbon is transported into subduction zones as an organic component (valence 0) in marine sediments or as carbonates (valence 4+) in altered oceanic basalts and/or veins in serpentinized mantle. During subduction, dissolution of carbonates by fluids produced by dehydration reactions enables the transport of carbonate and bicarbonate ions (valence 4+) in fluid inclusions trapped by eclogite minerals into depths (Frezzotti et al., 2011). Also the occurrence of CH_4 (valence 4–) in fluid inclusions preserved in subducted eclogites (Fu et al., 2003) further indicates that redox processes define the speciation of carbon (in these examples), as well as of other redox-sensitive elements in complex systems. The case of carbon speciation in subducted rocks and/or fluids is emblematic, since its valence state is likely governed (buffered) by the oxidation state of the host system. Subducted oceanic crust (eclogite) and serpentinites contain considerable amounts of iron so that the equilibria between ferric (Fe^{3+}) and ferrous (Fe^{2+}) iron in mineral assemblages are considered to buffer the oxygen fugacity (fO_2) and the valence state of carbon. On the other hand, the C species in subduction fluids may control the oxidation state of their hosting phase assemblages by redox reactions during degassing, dehydration, melting, and fluid/rock interactions. In other words, the dilemma of "what controls what" can be overcome only by considering the degree of fluid/rock interaction.

The oxidizing or reducing capacity of a rock is determined by the amount and by the oxidation state of redox-sensitive elements present (Evans, 2006). As a consequence, the fO_2, expressed as ΔFMQ ($\log fO_2$[sample] – $\log fO_2$ [fayalite-magnetite-quartz] to compare with different P-T equilibration conditions of the mineral assemblages), is likely very inhomogeneous in a subducting slab, reflecting the different bulk chemical-mineralogical compositions of the slab lithologies (Tumiati et al., 2015). Figure 6 attempts to picture this concept summarizing most of the data available in the literature. As we have seen previously, abyssal serpentinites represent the hydration of oceanic peridotites by seafloor hydrothermal and seawater alteration. According to Deschamps et al. (2013) and references cited in their work, these rocks record ΔfO_2 in the range between FMQ-2 and FMQ. Subducted serpentinites, originating either from abyssal peridotites or from the oceanic-continent transition zone, look slightly more reduced, with ΔfO_2 between FMQ-2 and FMQ-1. Prograde metamorphism of subducted serpentinites triggers the antigorite breakdown, with consequent H_2O release and growth of Fe^{2+}-bearing orthopyroxene, chlorite, and olivine. The crystallization of hematite in harzburgites studied by Debret et al. (2015) yields to a fO_2 increase in the slab up to ΔFMQ = +4. Finally, the antigorite-free subducted lithospheric mantle at depths of 150–350 km is generally more reduced (FMQ-2 to FMQ-3) even if more oxidized when compared with the surrounding mantle (Foley, 2011).

The subducted oceanic crust is depicted in Figure 6 as simplified blueschist to eclogite mafic rocks (blending blue and purple). Slab blueschist from South Tianshan (Li et al., 2016) and eclogite from North Qilian (Cao et al., 2011) in China record values of ΔFMQ from 0 to +4 and from FMQ<0 to FMQ+2.5, respectively.

Many more complications arise when we consider the slab-mantle interface. Mélange complexes are the result of deformation, boudinage, and chemical re-homogenization among the various lithologies derived from both slab and mantle scraps. The fluid-present high strain rates promote rock hybridization, which may act as chromatographic filtering, fixing, or releasing elements at variable P-T conditions (Schmidt and Poli, 2014). In this frame, slices from the slab and from the supra-subduction mantle embedded in this subduction mélange appear variously oxidized, likely due to the different fluid/rock ratio experienced. The ΔFMQ of blueschists and serpentinites ranges from –1 to +1 (Deschamps et al., 2013; Li et al., 2016), while hydrated eclogites reach up to +4.5 (Mattinson et al., 2004). The highest fO_2 variation is recorded by metapelitic rocks because they are characterized by variable bulk compositions. Eclogite-facies carbonate and calc-silicate rocks from Lindàs Nappe and Bergen Arcs (Norway) show fO_2 from FMQ+2 to FMQ+4 (Donohue and Essene, 2000; Boundy et al., 2002). Mn-bearing quartzite and metacherts range from FMQ+1 (Frezzotti et al., 2014) to FMQ+12 (Tumiati et al., 2015). As already pointed out by Evans (2012) and demonstrated by Malaspina et al. (2009b)

Downloaded from http://pubs.geoscienceworld.org/gsa/geosphere/article-pdf/14/6/2311/4578874/2311.pdf
by guest

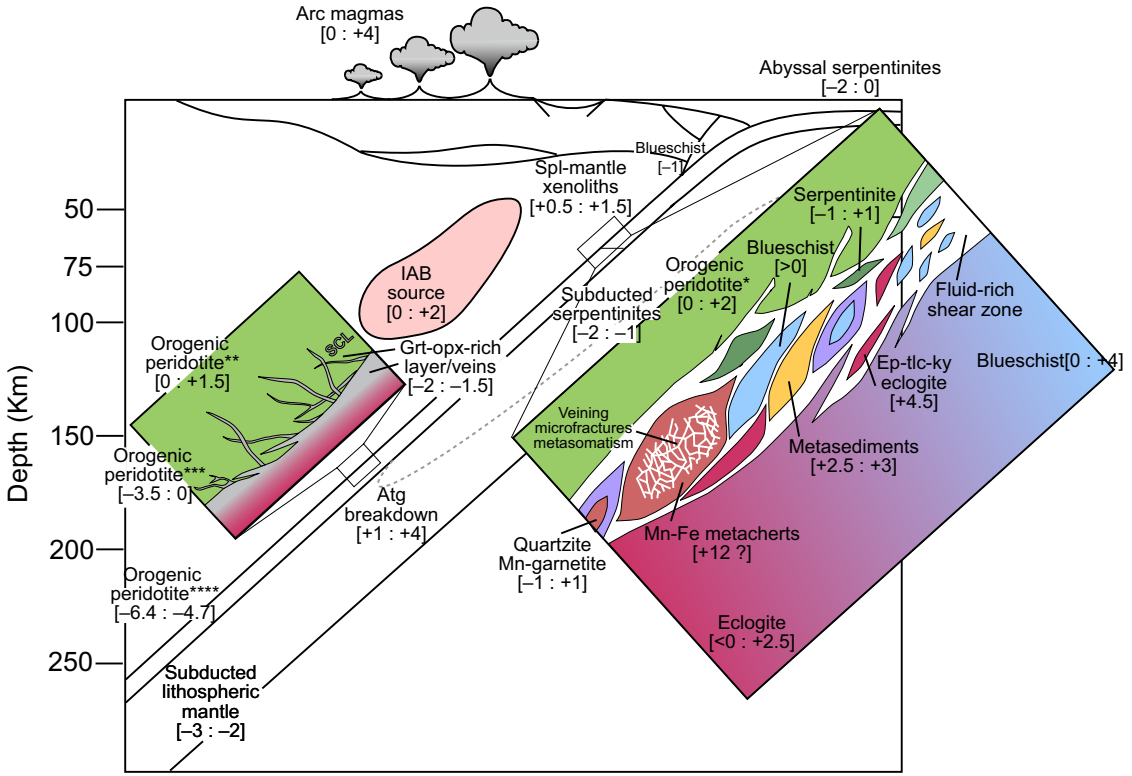

Figure 6. Schematic cartoon showing various redox conditions of subducted oceanic lithosphere and supra-subduction mantle. Numbers in brackets are the values of ΔFMQ. For comparison, the oxygen fugacities of arc magmas (Rohrbach et al., 2005; Carmichael et al., 2006; Evans et al., 2008) and island arc basalt (IAB) sources (Ballhaus, 1993; Parkinson and Arculus, 1999) are also reported. References: abyssal and subducted serpentinites (Deschamps et al., 2013), antigorite breakdown (Debret et al., 2015), subducted lithospheric mantle (Foley, 2011), accretionary prism blueschists (Zanchetta et al., 2018), slab blueschists and eclogites (Cao et al., 2011; Li et al., 2016); mélange lithotypes: serpentinites (Deschamps et al., 2013), blueschists (Li et al., 2016), metasediments (Donohue and Essene, 2000; Boundy et al., 2002), ep-tlc-ky eclogites (Mattinson et al., 2004), Mn-Fe metacherts (Tumiati et al., 2015), quartzite and Mn-garnetite (Frezzotti et al., 2014); slab-mantle interface: grt-opx-rich layer/veins (Malaspina et al., 2017); supra-subduction mantle: spl-mantle xenoliths (Brandon and Draper, 1996; Parkinson and Arculus, 1999; Peslier et al., 2002); *—orogenic peridotite from Ulten Zone (Malaspina et al., 2009a), grt-opx-rich layer/veins (Malaspina et al., 2017); **—orogenic peridotite from Sulu (Malaspina et al., 2009b); *—orogenic peridotite from Bardane (Malaspina et al., 2010; Rielli et al., 2017); ****—orogenic peridotite from Ugelvik (Rielli et al., 2017). SCL—supercritical liquid.**

and Tumiati et al. (2015), the oxidized or reduced nature of a rock, particularly in geodynamic environments where different bulk compositions and metasomatic chemical variations occur (e.g., subduction mélange), cannot be described by the commonly used intensive variables fO_2 or μO_2. Such variables are in fact by definition independent on the relative proportion of the phases in a rock (Frost, 1991). The estimate of an oxygen mass balance is therefore mandatory to evaluate the oxidation state of an equilibrium phase assemblage.

SLAB-TO-MANTLE MASS TRANSFER: TRACE ELEMENTS AND REDOX BUDGET

One of the most important pieces of evidence of the deep element recycling at subduction zones is the production of arc lavas relatively enriched in water, LILE, and to a lesser extent also in LREE, compared to the oceanic crust formed at mid-ocean ridges (Pearce et al., 2005). Such enrichment is called the "slab signature" (Tatsumi and Eggins, 1997). Moreover, the H_2O content and slab-derived fluid mobile elements of lavas and melt inclusions from arc volcanoes can be linearly correlated with their $Fe^{3+}/\Sigma Fe$, indicating that the oxidation state of such magmas is closely related to subduction fluid influx in their source (Kelley and Cottrell, 2009). If pure water is not likely an efficient carrier of Fe^{3+} (Schneider and Eggler, 1986), solute-rich slab-derived fluids could be potentially able to mobilize Fe^{3+} (Kelley and Cottrell, 2009) as they do for other trivalent fluid-immobile elements such as REE (Kessel et al., 2005a, 2005b; Tsay et al., 2014).

Several models have been proposed to explain how these geochemical signatures may be transferred from the slab to the arc lava sources in the mantle wedge (Tatsumi, 1986; Malaspina et al., 2006a, 2006b; Bebout, 2007; Hack and Thompson, 2011; Behn et al., 2011; Marschall and Schumacher, 2012; Till et al., 2012; Tumiati et al., 2013; Cannaò et al., 2015; Pirard and Hermann, 2015; Scambelluri et al., 2015). The formation of subduction channels play an important role for mass transfer at subduction zones between the subducting slab and the overlying mantle by percolation of slab fluids (Cloos, 1982; Bostock et al., 2002; Gerya et al., 2002). At pressures up to 3 GPa, the slab-mantle interface corresponds to a mélange zone (e.g., Bebout, 2007), where high fluid fluxes

Downloaded from http://pubs.geoscienceworld.org/gsa/geosphere/article-pdf/14/6/2311/4578874/2311.pdf
by guest

allow chemical exchange within the mélange materials forming hydrated and low-viscosity layers atop the subducting plate, with a hybrid geochemical signature (Bebout, 2007; Bostock, 2013).

The experimental work of Pirard and Hermann (2015) suggests that, at higher pressures, the direct transport of hydrous silicate-rich liquids by focused flow is the fastest and suitable mechanism of mass transfer through the mantle wedge able to supply the required geochemical signatures found in arc lavas worldwide. On the contrary, the percolation of supercritical liquids (*l.s.*) in mantle wedge peridotites by porous flow processes leads to the formation of several hydrous phases, such as amphibole and phlogopite (Zanetti et al., 1999; Scambelluri et al., 2006), which are able to incorporate significant quantities of trace elements, thus modifying the original slab signature (Pirard and Hermann, 2015). The SiO_2-enriched composition of supercritical liquids makes them very reactive with the overlying mantle, leading to the possible formation of metasomatic orthopyroxenite layers (Malaspina et al., 2006b; Endo et al., 2015).

Alternatively to the conventional model of mass transfer described above, Nielsen and Marschall (2017) propose that the slab signature may be transferred to arc lavas by mixing the solid components along the slab-mantle interface (see also Marschall and Schumacher, 2012; Cruz-Uribe et al., 2018), rising in the denser mantle as cold diapirs. Therefore, altered oceanic lithosphere, ophicarbonates, hybrid rocks from mélange zones, and hydrated peridotites drive the cold plume in the mantle wedge (Tumiati et al., 2013). The interaction between melts produced by the uprising cold plume and the mantle wedge may provide the fractionated trace-element signatures shown by arc volcanic rocks (Marschall and Schumacher, 2012; Spandler and Pirard, 2013; Nielsen and Marschall, 2017).

The mechanism of fluid-mediated redox budget transfer from the subducting plate to the overlying mantle, and then to the source regions of arc lavas in the mantle wedge, is still debated and poorly constrained. As discussed by Evans (2012), the oxidized forms of iron, sulfur, and carbon are potentially the agents able to transfer O^{2-} to the mantle, depending on their solubility in slab-derived fluid phases. Sulfur is probably the best carrier of redox budget (up to 1.6×10^{12} mol yr^{-1} from calculations by Evans, 2012) able to largely oxidize the Fe^{2+} of mantle mineral assemblages. Its transfer from the slab to the mantle is likely fluid mediated, since anyhdrite can be easily solubilized in saline fluids (Newton and Manning, 2005). Sulfate minerals are common daughter crystals in saline fluid inclusions of eclogite veins and coesite-bearing schists in the Western Alps (Philippot and Selverstone, 1991; Philippot et al., 1995), and in multiphase solid inclusions in UHP rocks from different terranes (see Table 1 of Frezzotti and Ferrando, 2015). If slab-derived fluids are able to transport sulfates in the overlying mantle, their reduction to sulfides will oxidize the Fe^{2+}-bearing minerals with a ratio of 1:8, if the oxygen fugacity of the mantle is below the sulfide-sulfur oxide buffer (Kelley and Cottrell, 2009). Also carbon can be a carrier of redox budget when transferred from the subducting plate to the overlying mantle after dissolution of carbonates in subduction fluids. Natural, theoretical, and experimental works demonstrated that both carbonates and CO_2 can be solubilized in HP fluids (Newton and Manning, 2002; Caciagli and Manning, 2003; Dolejš and Manning, 2010; Frezzotti et al., 2011; Ferrando et al., 2017; Tumiati et al., 2017). The conversion from CO_2 to C in the mantle gives a potential redox budget flux in the order of 10^{11} mol $year^{-1}$, inducing the oxidation of the sub-arc mantle (Evans, 2012). The solubility of Fe^{3+} in subduction zone fluids is not well known, even if the solute content of deep slab fluids may contain high Fe^{3+} concentrations also after the interaction with the host mineral during the crystallization of the daughter phases (Campione et al., 2017; Malaspina et al., 2017).

In geodynamic settings where a high fluid/rock ratio is expected, such as subduction mélanges, oxygen is likely transported along fractures and veins, possibly through mechanisms of dissolution-reprecipitation of O-enriched oxides and silicates (Tumiati et al., 2015) or by advective processes (Marschall and Schumacher, 2012; Tumiati et al., 2013; Nielsen and Marschall, 2017). On the other hand, fluid percolation at low fluid/rock ratios occurs when the metasomatic fluid phases produced at UHP (silica-saturated supercritical liquids) interact with peridotitic rocks at the slab-mantle interface (Fig. 6). In such occurrences, O_2 cannot be considered a perfectly mobile component, as defined by Korzhinskii (1959, 1965), because most of the redox reactions take place between solid oxides and silicates. Based on this principle, the quantity of inert components (e.g., FeO then forming Fe_2O_3 and vice versa) has a fundamental role, and the molar quantity of exchanged oxygen (nO_2) must be considered as an independent state variable. A recent study by Malaspina et al. (2017) reports the oxygen mass balance of crust-derived fluids preserved in multiphase solid inclusions from hybrid garnet orthopyroxenites of Maowu, a well-known example of metasomatic layers at the slab/mantle interface (Malaspina et al., 2006b; Chen et al., 2017). Because mass transfer is supported by chemical gradients, in this case by gradient in nO_2, a metasomatic front may develop from an oxidized slab, contributing to 200 mol m^{-3} of excess O_2 to the overlying mantle (10 mol m^{-3} O_2), passing through a transitional layer of hybrid rocks (gray field in Fig. 6) with the same excess of oxygen. On the contrary, the redox budget of the crust-derived fluids (multiphase inclusions) records more oxidized conditions than the host rock, reaching up to 400 mol m^{-3} of nO_2 (Malaspina et al., 2017). This suggests that even if the solubility of Fe^{3+} in subduction fluid phases is not well known, C-S–free aqueous fluids still remain potential carriers of oxidized components when they escape the slab-mantle interface.

METASOMATISM AND IMPLICATIONS FOR THE REDOX STATE OF THE SUPRA-SUBDUCTION MANTLE

Information on deep metasomatism of the supra-subduction mantle can be gained by the study of UHP terranes that contain felsic rocks associated with metasomatized garnet peridotites. Such associations represent an ideal context to study the element exchange between crustal and mantle rocks at pressures corresponding to sub-arc depths. Even if the origin of many HP-UHP orogenic peridotites is still under debate, examples of supra-subduction peridotites dragged by the subducting continental crust crop out in the Ulten Zone (Italian Central Alps), in the Western Gneiss Region (Norway), in the Massif Central

Downloaded from http://pubs.geoscienceworld.org/gsa/geosphere/article-pdf/14/6/2311/4578874/2311.pdf
by guest

and South Carpathian Variscides, in the Bohemian Massif, and in the Chinese Sulu Belt (Bodinier and Godard, 2013, and references therein). Most of these garnet peridotites provide evidence of recycling in the mantle of slab-derived fluids by the occurrence of primary multiphase solid inclusions, which have been attributed to silicate-rich supercritical liquids (van Roermund et al., 2002; Malaspina et al., 2006b; Vrijmoed et al., 2006; Scambelluri et al., 2008; Malaspina et al., 2010; Malaspina and Tumiati, 2012; Frezzotti and Ferrando, 2015). The trace-element pattern of the fluids that potentially leave the slab-mantle interface (the "residual fluid" of Malaspina et al., 2006b) is characterized by an enrichment of LREE and a selective enrichment in LILE, with spikes of Cs, Ba, and Pb relative to Rb and K. The pattern of this "residual fluid," reported in Figure 7 (Maowu fluid inclusions), resembles the LILE-enriched trace-element pattern of arc lavas, attributed to the addition of a "subduction component" that derives from the subducted sediments. Figure 7 also shows, for comparison, the incompatible trace-element pattern of peridotites from the Ulten Zone (Italian Alps), a known example of supra-subduction mantle peridotites metasomatized by crust-derived fluid phases at eclogite-facies conditions (Tumiati et al., 2003, 2007; Scambelluri et al., 2006). The patterns reported in Figure 7 record the transformation of lithospheric spinel lherzolites into garnet + amphibole and amphibole peridotites during a continuous P-T history (see also Nimis and Morten, 2000; Tumiati et al., 2003). They show a peculiar "W-type" signature with strong enrichment in Cs, Ba, Pb, and U with respect to Rb, K, and Th, coupled with moderate enrichment in Li (Fig. 7). The pattern of the "residual fluid" is also compared with that of pseudosecondary multiphase inclusions found in the garnet peridotites from Sulu, again another famous example of metasomatized supra-subduction mantle. Such inclusions were considered to represent a fluid phase that infiltrated the mantle after an earlier metasomatism by alkaline melt (Malaspina et al., 2009a). These inclusions have trace-element compositions surprisingly similar to the ones of Maowu (Fig. 7), pointing to a genetic relation with the two fluids. The similarity between the fluids trapped in the inclusions of both Maowu and Sulu peridotites and the metasomatic pattern recorded by the Ulten peridotites strongly suggests that these kinds of fluids may be effective metasomatic agents in the lithospheric supra-subduction mantle, once they escape the slab-mantle interface.

Crust-derived fluid metasomatism is also recorded by ultradeep majorite-bearing peridotites and websterites from Fjørtoft Island (Bardane, Western Gneiss Region). As demonstrated by Scambelluri et al. (2010), the mineral paragenesis re-equilibrated during deep Caledonian subduction is enriched in LREE, LILE (Pb, U, and Th), and light elements (Li and B). In particular, phlogopite and clinopyroxene and also majoritic garnet filling veins formed by percolating fluids at 6.5–7.0 GPa are the LREE and LILE repositories (Scambelluri et al., 2008). This indicates a common genesis from incompatible element-enriched subduction fluids that flushed the Bardane websterite (Scambelluri et al., 2010).

The Sr isotopic composition of these peridotites helps to further constrain the origin of fluids responsible for their metasomatism. The $^{87}Sr/^{86}Sr$ of the Sulu garnet peridotites, the Maowu garnet orthopyroxenite, Ulten zone

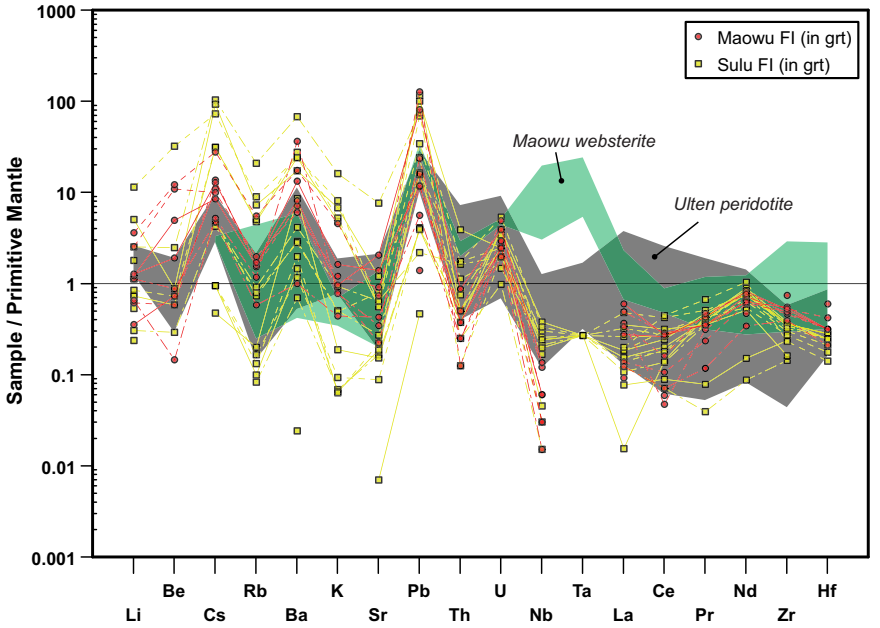

Figure 7. Primitive mantle (McDonough and Sun, 1995) normalized trace-element patterns of metasomatized supra-subduction zone mantle rocks (Ulten: Scambelluri et al., 2006; Maowu: Malaspina et al., 2006b) and fluid inclusions (FI) from Sulu (Malaspina et al., 2009a) and Maowu (Malaspina et al., 2006b).

Downloaded from http://pubs.geoscienceworld.org/gsa/geosphere/article-pdf/14/6/2311/4578874/2311.pdf
by guest

peridotites, and some of the peridotites from Norway reported in the literature point to a crust-derived metasomatism. As portrayed in Figure 8, they show enrichment in the radiogenic component, ranging from 0.7072 to 0.7076 for the Maowu orthopyroxenites (Jahn et al., 2003) and from 0.7085 to 0.7095 for the Sulu peridotites (Yang and Jahn, 2000). The peridotites from the Ulten zone show radiogenic $^{87}Sr/^{86}Sr$ signatures ranging from 0.7050 to 0.7074 (Tumiati et al., 2003), as well as some of the garnet peridotites from Norway (up to 0.7130; Spengler et al., 2009). These ranges provide evidence of the resetting of the original mantle isotopic signature (of 0.7025) toward crustal values (dashed dark blue field in Fig. 8). Together with Sr isotopes, Nd systematic also shows evidence of crustal contamination for some terranes, showing negative ε_{Nd} ranging from –4.2 to –7.1 for Maowu rocks, from –9.0 to –9.7 for Sulu peridotites, and down to –8.1 for the Ulten peridotites.

The Oxidation State of (Portions of) the Metasomatized Supra-Subduction Mantle

The three examples of mantle-derived garnet peridotites and websterites from Ulten, Sulu, and Bardane presented in the previous section also experienced metasomatism by ±C-bearing subduction fluid phases, up to 200 km depth. Ulten garnet peridotites were metasomatized by slab-derived fluids, which enhanced the crystallization of pargasitic amphibole and dolomite (Sapienza et al., 2009; Malaspina and Tumiati, 2012). Sulu peridotites record a multistage metasomatism by alkali-rich silicate melt, and a subsequent influx of a slab-derived incompatible element and silicate-rich fluid, which crystallized phlogopite and magnesite (Malaspina et al., 2009b). Websterites from Bardane preserve remnants of crust-derived fluids that precipitated graphite/diamond + dolomite/magnesite + Cr-spinel + phlogopite/K-amphibole in multiphase inclusions hosted by majoritic garnet (van Roermund et al., 2002; Scambelluri et al., 2008; Malaspina et al., 2010). As we will see later, an apparent correlation between the composition of the metasomatic agent (C- and alkali-bearing) and the fluid-induced oxidation of the peridotite mineral assemblage may occur.

The interpretation of the oxygen fugacities retrieved from mantle rocks is still a subject of debate. Even though the works by Canil (2002) and Lee et al. (2005) emphasize a homogeneity in the redox state of the convective asthenosphere, including subduction zone environments, systematic fO_2 estimates for mantle xenoliths from different geological settings, both in the spinel and garnet facies, indicate that the upper mantle is zoned (Daniels and Gurney, 1991; Ballhaus and Frost, 1994; Ballhaus, 1995; Woodland and Koch, 2003; Frost and McCammon, 2008). In addition, there are a number of studies in the literature that reveal lateral fO_2 variations related to different tectonic settings. These are summarized in Figure 9 (references are reported in the figure caption), where the range of oxygen fugacities (ΔFMQ) for spinel and garnet peridotites from various tectonic settings (black lines) are plotted as a function of equilibration pressure. These studies are in contrast to the "oxidized" nature of the mantle wedge, derived from oxygen thermobarometry of arc lavas (yellow lines) or from models of IAB sources (blue square).

For HP-UHP peridotite mineral assemblages, fO_2 can be evaluated from several equilibria involving Fe^{3+}-garnet components, where Fe^{3+} occurs in octahedral coordination. For the olivine + orthopyroxene + Fe^{3+}-garnet assemblage, two of these reactions are represented by:

(1) $2\ Ca_3Fe^{3+}{}_2Si_3O_{12} + 2\ Mg_3Al_2Si_3O_{12} + 2\ Fe_2Si_2O_6 = 2\ Ca_3Al_2Si_3O_{12} + 4Fe_2SiO_4 + 3\ Mg_2Si_2O_6 + O_2$

and

(2) $2\ Fe^{2+}{}_3Fe^{3+}{}_2Si_3O_{12}$ (skiagite) $= 4\ Fe_2SiO_4 + Fe_2Si_2O_6 + O_2$.

Equilibrium (1) by Luth et al. (1990) has been experimentally tested by Stagno et al. (2013) at P > 5 GPa, while equilibrium (2) was calibrated by Gudmundsson and Wood (1995) and is valid at pressures below 5 GPa (Stagno et al., 2013). At high pressures, oxygen fugacity is therefore traditionally determined from the Fe^{3+} contents of garnet in equilibrium with olivine and orthopyroxene. The green (and gray) lines portrayed in Figure 9 are the ΔFMQ ranges cal-

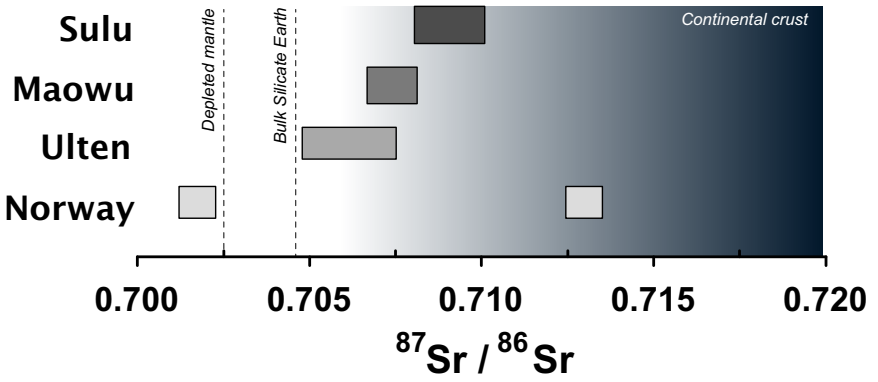

Figure 8. $^{87}Sr/^{86}Sr$ isotopic ratio of mantle rocks form supra-subduction setting. Sulu from Yang and Jahn (2000); Maowu from Jahn et al. (2003); Ulten from Tumiati et al. (2003); Norway from Spengler et al. (2009). Depleted mantle from Rehkämper and Hofmann (1997); bulk silicate earth from Salters and Stracke (2004). The dark-blue field represents the typical range of $^{87}Sr/^{86}Sr$ signature of the continental materials.

Downloaded from http://pubs.geoscienceworld.org/gsa/geosphere/article-pdf/14/6/2311/4578874/2311.pdf
by guest

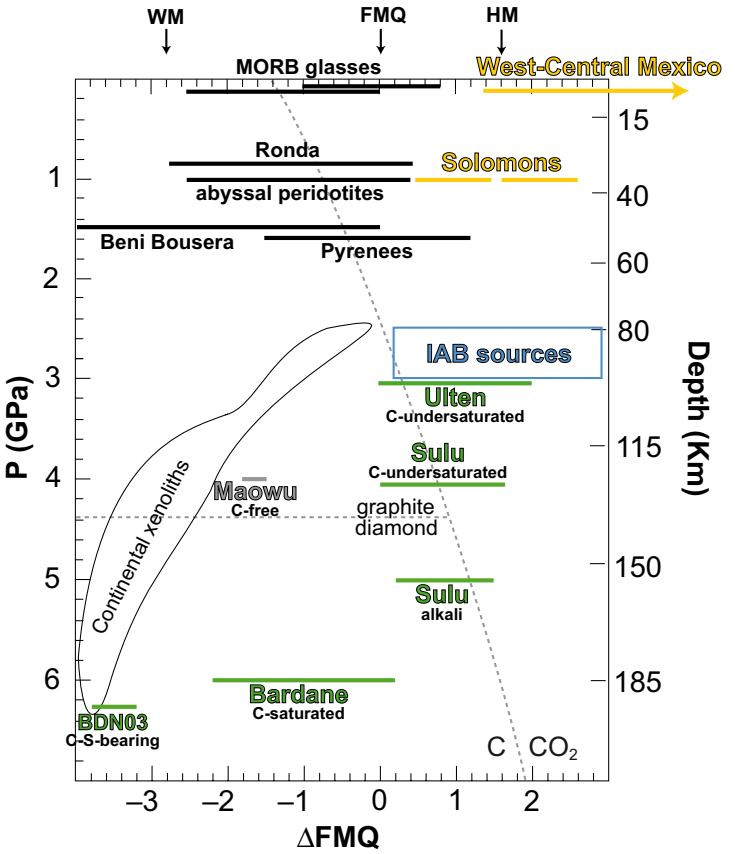

Figure 9. Ranges and average values of ΔFMQ = (logfO_2 sample – logfO_2 FMQ) for the Ulten, Maowu, Sulu, and Bardane garnet peridotites plotted as a function of pressure (data from Malaspina et al., 2009b, 2010, 2017; BDN03 is from Rielli et al., 2017). They are compared with selected examples of glasses and peridotites from various tectonic settings, equilibrated at similar temperature conditions: mid-ocean ridge basalt (MORB) glasses (Christie et al., 1986; Bézos and Humler, 2005), oceanic mantle lithosphere (Bryndzia and Wood, 1990), and peridotite massifs (Woodland et al., 1992, 2006) (black lines); garnet peridotite xenoliths from sub-cratonic mantle (Woodland and Koch, 2003) (white area). Note the negatively correlated trend between supra-subduction garnet peridotites (green lines), arc lavas from west-central Mexico (Carmichael et al., 2006), and from Solomon (Rohrbach et al., 2005) (yellow lines), and island arc basalt (IAB) sources (Ballhaus, 1993; Parkinson and Arculus, 1999), which is grossly parallel to the ΔFMQ decrease of continental xenoliths with depth. The CCO oxygen buffer (C = O_2+CO_2), calculated at an average T = 900 °C and the graphite-diamond transition at the temperature conditions of M3-3 stage of Bardane peridotites (1000 °C), are also indicated for reference. WM—wustite-magnetite; FMQ—fayalite-magnetite-quartz; and HM—hematite-magnetite buffers.

culated from Fe^{3+} measurements of garnets from supra-subduction orogenic peridotites, in relation to the metasomatic phase assemblages formed: C-free (Maowu), C-undersaturated (Ulten and Sulu), alkali-bearing (Sulu), C-S–saturated (Bardane), slab-derived fluids. Lee et al. (2005) interpreted the high barometric fO_2 of arc lavas as resulting from the evolution of magmas during their ascent, emplacement, and/or magmatic differentiation. These authors have also suggested that the generally higher fO_2 of mantle xenoliths from the arc lithosphere compared with the convective mantle at similar pressures (Christie et al., 1986; Bryndzia and Wood, 1990; Bézos and Humler, 2005) is likely due to continuous metasomatic fluid influx in these mantle rocks during their long residence time in the sub-arc lithosphere. Even if the dispute about the process responsible for the relative oxidation of the mantle at subduction zones and the actual oxidizing ability of slab-derived metasomatic fluids is still going on, the metasomatized mantle apparently looks more "oxidized."

Interestingly, the fO_2 calculated for the garnet + orthopyroxene ± olivine assemblage of the C-free metasomatic orthopyroxenites from Maowu (gray line in Fig. 9) shows much lower values with respect to that of supra-subduction C-bearing peridotites equilibrated at similar pressures. The data compilation reported in Figure 9 therefore suggests that carbon- (and sulfur-; Rielli et al., 2017) rich fluids may play an important role in the oxidation of iron-bearing garnets in mantle peridotites.

Besides the direct involvement of carbon and sulfur in fluid-mediated redox reactions in the mantle, we must consider that the increase of Fe^{3+} in garnet from mantle peridotites is not always correlated with the increase of the whole-rock Fe_2O_3, but could also be the consequence of the partitioning of Fe^{3+} from clinopyroxene into garnet (Canil and O'Neill, 1996; Woodland and Peltonen, 1999; Woodland and Koch, 2003; Rohrbach et al., 2007, 2011; Woodland, 2009). A recent work by Aulbach et al. (2017) also reports a strong negative correlation of $Fe^{3+}/\Sigma Fe$ in garnet with the jadeite content in coexisting clinopyroxene. This has been again interpreted as partitioning of Fe^{3+} from garnet into jadeite-rich clinopyroxene with consequences in the fO_2 calculations from garnet-only–bearing assemblages. Moreover, because redox reactions depend on the abundance of redox-sensitive elements, and on the moles of oxygen exchanged in the redox equilibria, the determination of the oxidation state of metasomatized garnet peridotites is a demanding task because clinopyroxene, amphibole, and phlogopite, in addition to garnet (and/or spinel), incorporate both ferric and ferrous iron (Malaspina et al., 2012, 2017).

Finally, another important underestimated aspect related to the metasomatic oxidation of garnet peridotites is the role of alkali elements, particularly of Na_2O. Clinopyroxene in metasomatized garnet peridotites may be enriched in Fe^{3+} as aegirine component (Woodland, 2009; Aulbach et al., 2017) and potentially become the major Fe^{3+} host when the peridotites are metasomatized by Fe_2O_3- and alkali-rich fluid phases, as was exactly what happened to Sulu peridotites during the first stage of metasomatism by alkali-rich melts (Fig. 9; Malaspina et al., 2012). This suggests that if net bulk oxidation can be demonstrated, carbon-, sulfur-, and also alkali-bearing slab-derived metasomatic agents may be potential carriers of S^{6+}/S^{3-}, C^{4+}, and Fe^{3+} capable of oxidizing the overlying mantle.

Downloaded from http://pubs.geoscienceworld.org/gsa/geosphere/article-pdf/14/6/2311/4578874/2311.pdf
by guest

CONCLUDING REMARKS

Based on the questions addressed in the beginning of this review, some concluding remarks are listed below.

(1) Geophysical imaging of subduction zones (e.g., Bostock et al., 2002) documents an important front of hydration in the supra-subduction mantle region, due to the uprise of fluids released from sediments and subducted oceanic crust. The hydration mechanism of the supra-subduction mantle produces different plate interface style settings depending on the thermal state of the subduction zone. This also plays an important role in the geochemical imprint of the hydrated mantle and its possible contribution to arc magmatism (Marschall and Schumacher, 2012; Spandler and Pirard, 2013). The released fluids developing mélange terrains promote the formation of "hybrid" rocks, which are able to selectively exchange trace elements with other slab reservoirs. The hybridization process may lead to a chemical transformation both in terms of major elements (e.g., formation of lawsonites, chlorite schists, and tourmaline-rich blackwalls; see Marschall et al., 2006; Marschall and Schumacher, 2012; Vitale Brovarone et al., 2014) and/or of trace elements. In top slab mélange, the prograde fluid-mediated chemical exchange between slices of slab and wedge-derived rocks and slab fluids can be tracked using fluid-mobile elements (e.g., As and Sb) and isotopic tracers (B, Sr, and Pb). This process may yield to oddities in the geochemical signature of mantle rocks.

(2) The major- and trace-element concentration of slab-derived fluids strongly depends on their partitioning with stable phase assemblages, which in turn depend on the thermal regime of subduction (Fig. 1). Phengite is the most important phase controlling the partitioning of LILE and LREE in K-bearing systems and is stable up to 200 km depth along cold subduction paths. In addition, accessory minerals such as allanite, monazite, zircon, and rutile, which are ubiquitous in different slab lithologies, play an important role in the storage of HFSE but also LREE and U-Th. The stability of garnet as a product of metamorphic reactions controls the partitioning of HREE. The release of incompatible elements, particularly of LILE and LREE, is modulated by the modal amount of key phases, such as phengite, in the slab rocks and by their stability, which depends on the occurrence of free H_2O, which lowers their solidus temperature (Fig. 1).

(3) The geochemical modification of the supra-subduction mantle wedge strongly depends on the magnitude of trace-element supply by fluids/melts. At relatively low pressures (up to 3 GPa, i.e., antigorite breakdown), the subducted lithosphere releases large quantities of H_2O and forms mélange layers characterized by high fluid/rock ratios. In this framework, elements are likely transported along fractures and veins (Fig. 6), possibly through mechanisms of dissolution-reprecipitation or by advective processes. At higher pressures (P > 3 GPa), fluid percolation at low fluid/rock ratios (porous or focused flow) is mediated by Si-saturated supercritical liquids interacting with peridotitic rocks at the slab-mantle interface. In such occurrences, focused flow is the fastest and most suitable mechanism of mass transfer through the mantle wedge capable of supplying the required geochemical signatures found in arc lavas.

(4) The redox state of the subducting lithosphere is intrinsically heterogeneous due to the different lithologies bearing different amounts of redox-sensitive elements (Fe, Mn, C, and S) and different fluid/rock ratios experienced (Fig. 6). The estimate of an oxygen mass balance is mandatory to evaluate the oxidation state of the slab equilibrium phase assemblages. Nevertheless, one of the most important pieces of evidence of the deep redox budget recycling at subduction zones is the production of arc lavas with $Fe^{3+}/\Sigma Fe$ linearly correlated with the H_2O content and slab-derived fluid mobile elements. This evidence indicates that the oxidation state of arc magmas is closely related to the transfer of Fe^{3+}, C^{4+}, and/or S^{6+} in their source by slab-derived metasomatic agents.

(5) The redox-state evolution of slab and supra-subduction lithologies may influence the speciation of elements in the metasomatic fluids infiltrating the overlying mantle. The valence state of carbon and sulfur and the speciation of their compounds are governed by the rock system, i.e., by the equilibria among mineral assemblages containing redox-sensitive major elements (e.g., Fe and Mn). Alternatively, the carbon and/or sulfur species in subducted rocks and deep fluids control the oxidation state of the host system by redox reactions during fluid/rock interactions (e.g., Fig. 9). Whether the redox state of the system is buffered by the rock or by C-S–bearing fluids depends on the fluid/rock ratios. At high ratios, such as mélange layers, fluids control the redox state of the system, and oxygen can be considered perfectly mobile. At low ratios, such as during porous flow of metasomatic agents at UHP, the mantle rock controls the speciation of redox-sensitive metasomatic components, and oxygen is considered inert. Finally, another important aspect related to the metasomatic-related oxidation of the mantle wedge is the role of alkali elements, particularly of Na_2O, which favors the incorporation of Fe^{3+} in peridotite clinopyroxene as aegirine component. This suggests that if net bulk oxidation can be demonstrated, C-, S-, and even alkali-bearing slab-derived metasomatic agents may oxidize the overlying mantle.

ACKNOWLEDGMENTS

This research was funded by the Italian Ministry of Education, Universities and Research (PRIN-COFIN project 2012R33ECR_002 Volatile transfer at convergent plate margins: Linking COH fluids/melts heterogeneities to tectonic anomalies in subduction zones). This work also benefited from the University of Milano Bicocca 2015-ATE-0218. The authors are indebted to Guest Associate Editor G.E. Bebout and S. Ferrando and an anonymous reviewer for their comments and thorough review of the manuscript.

Downloaded from http://pubs.geoscienceworld.org/gsa/geosphere/article-pdf/14/6/2311/4578874/2311.pdf
by guest

REFERENCES CITED

Allen, D.E., and Seyfried, W.E., 2005, REE controls in ultramafic hosted MOR hydrothermal systems: An experimental study at elevated temperature and pressure: Geochimica et Cosmochimica Acta, v. 69, p. 675–683, https://doi.org/10.1016/j.gca.2004.07.016.

Alt, J.C., and Teagle, D.A.H., 2003, Hydrothermal alteration of upper oceanic crust formed at a fast-spreading ridge: Mineral, chemical, and isotopic evidence from ODP Site 801: Chemical Geology, https://doi.org/10.1016/S0009-2541(03)00201-8.

Andreani, M., Mével, C., Boullier, A.M., and Escartín, J., 2007, Dynamic control on serpentine crystallization in veins: Constraints on hydration processes in oceanic peridotites: Geochemistry Geophysics Geosystems, v. 8, https://doi.org/10.1029/2006GC001373.

Arculus, R.J., Lapierre, H., and Jaillard, E., 1999, Geochemical window into subduction and accretion processes: Raspas metamorphic complex, Ecuador: Geology, v. 27, p. 547–550, https://doi.org/10.1130/0091-7613(1999)027<0547:GWISAA>2.3.CO;2.

Augustin, N., Paulick, H., Lackschewitz, K.S., Eisenhauer, A., Garbe-Schönberg, D., Kuhn, T., Botz, R., and Schmidt, M., 2012, Alteration at the ultramafic-hosted Logatchev hydrothermal field: Constraints from trace element and Sr-O isotope data: Geochemistry Geophysics Geosystems, v. 13, https://doi.org/10.1029/2011GC003903.

Aulbach, S., Woodland, A.B., Vasilyev, P., Galvez, M.E., and Viljoen, K.S., 2017, Effects of low-pressure igneous processes and subduction on Fe3+/ΣFe and redox state of mantle eclogites from Lace (Kaapvaal craton): Earth and Planetary Science Letters, v. 474, p. 283–295, https://doi.org/10.1016/j.epsl.2017.06.030.

Auzanneau, E., Vielzeuf, D., and Schmidt, M.W., 2006, Experimental evidence of decompression melting during exhumation of subducted continental crust: Contributions to Mineralogy and Petrology, v. 152, p. 125–148, https://doi.org/10.1007/s00410-006-0104-5.

Ballhaus, C., 1993, Redox states of lithospheric and asthenospheric upper mantle: Contributions to Mineralogy and Petrology, v. 114, p. 331–348, https://doi.org/10.1007/BF01046536.

Ballhaus, C., 1995, Is the upper mantle metal-saturated?: Earth and Planetary Science Letters, v. 132, p. 75–86, https://doi.org/10.1016/0012-821X(95)00047-G.

Ballhaus, C., and Frost, B.R., 1994, The generation of oxidized CO_2-bearing basaltic melts from reduced CH_4-bearing upper mantle sources: Geochimica et Cosmochimica Acta, v. 58, p. 4931–4940, https://doi.org/10.1016/0016-7037(94)90222-4.

Bebout, G.E., 2007, Metamorphic chemical geodynamics of subduction zones: Earth and Planetary Science Letters, v. 260, p. 373–393, https://doi.org/10.1016/j.epsl.2007.05.050.

Bebout, G.E., 2013, Chemical and Isotopic Cycling in Subduction Zones: Treatise on Geochemistry (second edition), v. 4, p. 703–747, https://doi.org/10.1016/B978-0-08-095975-7.00322-3.

Bebout, G.E., and Barton, M.D., 1993, Metasomatism during subduction: Products and possible paths in the Catalina Schist, California: Chemical Geology, v. 108, p. 61–92, https://doi.org/10.1016/0009-2541(93)90318-D.

Bebout, G.E., Ryan, J.G., Leeman, W.P., and Bebout, A.E., 1999, Fractionation of trace elements by subduction-zone metamorphism—Effect of convergent-margin thermal evolution: Earth and Planetary Science Letters, v. 171, p. 63–81, https://doi.org/10.1016/S0012-821X(99)00135-1.

Bebout, G.E., Bebout, A.E., and Graham, C.M., 2007, Cycling of B, Li, and LILE (K, Cs, Rb, Ba, Sr) into subduction zones: SIMS evidence from micas in high-P/T metasedimentary rocks: Chemical Geology, v. 239, p. 284–304, https://doi.org/10.1016/j.chemgeo.2006.10.016.

Bebout, G.E., Agard, P., Kobayashi, K., Moriguti, T., and Nakamura, E., 2013, Devolatilization history and trace element mobility in deeply subducted sedimentary rocks: Evidence from Western Alps HP/UHP suites: Chemical Geology, v. 342, p. 1–20, https://doi.org/10.1016/j.chemgeo.2013.01.009.

Becker, H., Jochum, K.P., and Carlson, R.W., 2000, Trace element fractionation during dehydration of eclogites from high-pressure terranes and the implications for element fluxes in subduction zones: Chemical Geology, v. 163, p. 65–99, https://doi.org/10.1016/S0009-2541(99)00071-6.

Behn, M.D., Kelemen, P.B., Hirth, G., Hacker, B.R., and Massonne, H.J., 2011, Diapirs as the source of the sediment signature in arc lavas: Nature Geoscience, v. 4, p. 641–646, https://doi.org/10.1038/ngeo1214.

Beltrando, M., Manatschal, G., Mohn, G., Dal Piaz, G.V., Vitale Brovarone, A., and Masini, E., 2014, Recognizing remnants of magma-poor rifted margins in high-pressure orogenic belts: The Alpine case study: Earth-Science Reviews, https://doi.org/10.1016/j.earscirev.2014.01.001.

Bézos, A., and Humler, E., 2005, The Fe3+/ΣFe ratios of MORB glasses and their implications for mantle melting: Geochimica et Cosmochimica Acta, v. 69, p. 711–725, https://doi.org/10.1016/j.gca.2004.07.026.

Biino, G.G., and Compagnoni, R., 1992, Very-High Pressure Metamorphism of the Brossasco Coronite Metagranite, Southern Dora-Maira-Massif, Western Alps: Schweizerische Mineralogische und Petrographische Mitteilungen, v. 72, p. 347–362.

Blanco-Quintero, I.F., Proenza, J.A., García-Casco, A., Tauler, E., and Galí, S., 2011, Serpentinites and serpentinites within a fossil subduction channel: La Corea mélange, eastern Cuba: Geologica Acta, v. 9, p. 389–405, https://doi.org/10.1344/105.00000166.

Bodinier, J.L., and Godard, M., 2013, Orogenic, Ophiolitic, and Abyssal Peridotites: Treatise on Geochemistry (second edition), v. 3, p. 103–167, https://doi.org/10.1016/B978-0-08-095975-7.00204-7.

Bonatti, E., 1976, Serpentinite protrusions in the oceanic crust: Earth and Planetary Science Letters, v. 32, p. 107–113, https://doi.org/10.1016/0012-821X(76)90048-0.

Boschi, C., Dini, A., Früh-Green, G.L., and Kelley, D.S., 2008, Isotopic and element exchange during serpentinization and metasomatism at the Atlantis Massif (MAR 30°N): Insights from B and Sr isotope data: Geochimica et Cosmochimica Acta, v. 72, p. 1801–1823, https://doi.org/10.1016/j.gca.2008.01.013.

Bostock, M.G., 2013, The Moho in subduction zones: Tectonophysics, v. 609, p. 547–557, https://doi.org/10.1016/j.tecto.2012.07.007.

Bostock, M.G., Hyndman, R.D., Rondenay, S., and Peacock, S.M., 2002, An inverted continental moho and serpentinization of the forearc mantle: Nature, v. 417, p. 536–538, https://doi.org/10.1038/417536a.

Boundy, T.M., Donohue, C.L., Essene, E.J., Mezger, K., and Austrheim, H., 2002, Discovery of eclogite facies carbonate rocks from the Lindås Nappe, Caledonides, Western Norway: Journal of Metamorphic Geology, v. 20, p. 649–667, https://doi.org/10.1046/j.1525-1314.2002.00396.x.

Brandon, A.D., and Draper, D.S., 1996, Constraints on the origin of the oxidation state of mantle overlying subduction zones: An example from Simcoe, Washington, USA: Geochimica et Cosmochimica Acta, v. 60, p. 1739–1749, https://doi.org/10.1016/0016-7037(96)00056-7.

Bruland, K.W., Middag, R., and Lohan, M.C., 2013, Controls of Trace Metals in Seawater: Treatise on Geochemistry (second edition), v. 8, p. 19–51, https://doi.org/10.1016/B978-0-08-095975-7.00602-1.

Bryndzia, L.T., and Wood, B.J., 1990, Oxygen thermobarometry of abyssal spinel peridotites: The redox state and C-O-H volatile composition of the Earth's sub-oceanic upper mantle: The American Mineralogist, v. 290, p. 1093–1116.

Busigny, V., Cartigny, P., Philippot, P., Ader, M., and Javoy, M., 2003, Massive recycling of nitrogen and other fluid-mobile elements (K, Rb, Cs, H) in a cold slab environment: Evidence from HP to UHP oceanic metasediments of the Schistes Lustrés nappe (western Alps, Europe): Earth and Planetary Science Letters, v. 215, p. 27–42, https://doi.org/10.1016/S0012-821X(03)00453-9.

Caciagli, N.C., and Manning, C.E., 2003, The solubility of calcite in water at 6–16 kbar and 500–800 °C: Contributions to Mineralogy and Petrology, v. 146, p. 275–285, https://doi.org/10.1007/s00410-003-0501-y.

Campione, M., Tumiati, S., and Malaspina, N., 2017, Primary spinel + chlorite inclusions in mantle garnet formed at ultrahigh-pressure: Geochemical Perspectives Letters, v. 4, p. 19–23, https://doi.org/10.7185/geochemlet.1730.

Canil, D., 2002, Vanadium in peridotites, mantle redox and tectonic environments: Archean to present: Earth and Planetary Science Letters, v. 195, p. 75–90, https://doi.org/10.1016/S0012-821X(01)00582-9.

Canil, D., and O'Neill, H.S.C., 1996, Distribution of ferric iron in some upper-mantle assemblages: Journal of Petrology, v. 37, p. 609–635, https://doi.org/10.1093/petrology/37.3.609.

Cannaò, E., Agostini, S., Scambelluri, M., Tonarini, S., and Godard, M., 2015, B, Sr and Pb isotope geochemistry of high-pressure Alpine metaperidotites monitors fluid-mediated element recycling during serpentinite dehydration in subduction mélange (Cima di Gagnone, Swiss Central Alps): Geochimica et Cosmochimica Acta, v. 163, p. 80–100, https://doi.org/10.1016/j.gca.2015.04.024.

Cannaò, E., Scambelluri, M., Agostini, S., Tonarini, S., and Godard, M., 2016, Linking serpentinite geochemistry with tectonic evolution at the subduction plate-interface: The Voltri Massif case study (Ligurian Western Alps, Italy): Geochimica et Cosmochimica Acta, v. 190, p. 115–133, https://doi.org/10.1016/j.gca.2016.06.034.

Cao, Y., Song, S.G., Niu, Y.L., Jung, H., and Jin, Z.M., 2011, Variation of mineral composition, fabric and oxygen fugacity from massive to foliated eclogites during exhumation of subducted ocean crust in the North Qilian suture zone, NW China: Journal of Metamorphic Geology, v. 29, p. 699–720, https://doi.org/10.1111/j.1525-1314.2011.00937.x.

Downloaded from http://pubs.geoscienceworld.org/gsa/geosphere/article-pdf/14/6/2311/4578874/2311.pdf
by guest

Carmichael, I.S.E., Frey, H.M., Lange, R.A., and Hall, C.M., 2006, The Pleistocene cinder cones surrounding Volcán Colima, Mexico re-visited: Eruption ages and volumes, oxidation states, and sulfur content: Bulletin of Volcanology, v. 68, p. 407–419, https://doi.org/10.1007/s00445-005-0015-8.

Carter, L.B., Skora, S., Blundy, J.D., De Hoog, J.C.M., and Elliott, T., 2015, An experimental study of trace element fluxes from subducted oceanic crust: Journal of Petrology, v. 56, p. 1585–1606, https://doi.org/10.1093/petrology/egv046.

Chalot-Prat, F., Ganne, J., and Lombard, A., 2003, No significant element transfer from the oceanic plate to the mantle wedge during subduction and exhumation of the Tethys lithosphere (Western Alps): Lithos, v. 69, p. 69–103, https://doi.org/10.1016/S0024-4937(03)00047-1.

Chen, Y., Su, B., and Chu, Z., 2017, Modification of an ancient subcontinental lithospheric mantle by continental subduction: Insight from the Maowu garnet peridotites in the Dabie UHP belt, eastern China: Lithos, v. 278–281, p. 54–71, https://doi.org/10.1016/j.lithos.2017.01.025.

Chopin, C., 1984, Coesite and pure pyrope in high-grade blueschists of the Western Alps: A first record and some consequences: Contributions to Mineralogy and Petrology, v. 86, p. 107–118, https://doi.org/10.1007/BF00381838.

Christie, D.M., Carmichael, I.S.E., and Langmuir, C.H., 1986, Oxidation states of mid-ocean ridge basalt glasses: Earth and Planetary Science Letters, v. 79, p. 397–411, https://doi.org/10.1016/0012-821X(86)90195-0.

Cloos, M., 1982, Flow mélanges: Numerical modeling and geologic constraints on their origin in the Franciscan subduction complex, California: Geological Society of America Bulletin, v. 93, p. 330–345, https://doi.org/10.1130/0016-7606(1982)93<330:FMNMAG>2.0.CO;2.

Collins, N.C., Bebout, G.E., Angiboust, S., Agard, P., Scambelluri, M., Crispini, L., and John, T., 2015, Subduction zone metamorphic pathway for deep carbon cycling: II. Evidence from HP/UHP metabasaltic rocks and ophicarbonates: Chemical Geology, https://doi.org/10.1016/j.chemgeo.2015.06.012.

Compagnoni, R., Hirajima, T., and Chopin, C., 1995, Ultra-high-pressure metamorphic rocks in the Western Alps, *in* Coleman, R.G., and Wang, X., eds., Ultrahigh Pressure Metamorphism: Cambridge University Press, p. 206–243, https://doi.org/10.1017/CBO9780511573088.008.

Cruz-Uribe, A.M., Marschall, H.R., Gaetani, G.A., and Le Roux, V., 2018, Generation of alkaline magmas in subduction zones by partial melting of mélange diapirs—An experimental study: Geology, v. 46, no. 4, p. 343–346, https://doi.org/10.1130/G39956.1.

Dal Piaz, G., 1999, The Austroalpine-Piedmont nappe stack and the puzzle of Alpine Tethys: Memorie di Scienze Geologiche Padova, v. 51, p. 155–176.

Daniels, L.R.M., and Gurney, J.J., 1991, Oxygen fugacity constraints on the southern African lithosphere: Contributions to Mineralogy and Petrology, v. 108, p. 154–161, https://doi.org/10.1007/BF00307334.

Debret, B., Andreani, M., Godard, M., Nicollet, C., Schwartz, S., and Lafay, R., 2013, Trace element behavior during serpentinization/de-serpentinization of an eclogitized oceanic lithosphere: A LA-ICPMS study of the Lanzo ultramafic massif (Western Alps): Chemical Geology, v. 357, p. 117–133, https://doi.org/10.1016/j.chemgeo.2013.08.025.

Debret, B., Bolfan-Casanova, N., Padrón-Navarta, J.A., Martin-Hernandez, F., Andreani, M., Garrido, C.J., López Sánchez-Vizcaíno, V., Gómez-Pugnaire, M.T., Muñoz, M., and Trcera, N., 2015, Redox state of iron during high-pressure serpentinite dehydration: Contributions to Mineralogy and Petrology, v. 169, https://doi.org/10.1007/s00410-015-1130-y.

Debret, B., Koga, K.T., Cattani, F., Nicollet, C., Van den Bleeken, G., and Schwartz, S., 2016, Volatile (Li, B, F and Cl) mobility during amphibole breakdown in subduction zones: Lithos, v. 244, p. 165–181, https://doi.org/10.1016/j.lithos.2015.12.004.

Delacour, A., Früh-Green, G.L., Frank, M., Gutjahr, M., and Kelley, D.S., 2008, Sr- and Nd-isotope geochemistry of the Atlantis Massif (30°N, MAR): Implications for fluid fluxes and lithospheric heterogeneity: Chemical Geology, v. 254, p. 19–35, https://doi.org/10.1016/j.chemgeo.2008.05.018.

Deschamps, F., Guillot, S., Godard, M., Andreani, M., and Hattori, K., 2011, Serpentinites act as sponges for fluid-mobile elements in abyssal and subduction zone environments: Terra Nova, v. 23, p. 171–178, https://doi.org/10.1111/j.1365-3121.2011.00995.x.

Deschamps, F., Godard, M., Guillot, S., Chauvel, C., Andreani, M., Hattori, K., Wunder, B., and France, L., 2012, Behavior of fluid-mobile elements in serpentines from abyssal to subduction environments: Examples from Cuba and Dominican Republic: Chemical Geology, v. 312, p. 93–117, https://doi.org/10.1016/j.chemgeo.2012.04.009.

Deschamps, F., Godard, M., Guillot, S., and Hattori, K., 2013, Geochemistry of subduction zone serpentinites: A review: Lithos, v. 178, p. 96–127, https://doi.org/10.1016/j.lithos.2013.05.019.

Dolejš, D., and Manning, C.E., 2010, Thermodynamic model for mineral solubility in aqueous fluids: Theory, calibration and application to model fluid-flow systems: Geofluids, v. 10, p. 20–40, https://doi.org/10.1111/j.1468-8123.2010.00282.x.

Domanik, K.J., and Holloway, J.R., 1996, The stability and composition of phengitic muscovite and associated phases from 5.5 to 11 GPa: Implications for deeply subducted sediments: Geochimica et Cosmochimica Acta, v. 60, p. 4133–4150, https://doi.org/10.1016/S0016-7037(96)00241-4.

Donohue, C.L., and Essene, E.J., 2000, An oxygen barometer with the assemblage garnet-epidote: Earth and Planetary Science Letters, v. 181, p. 459–472, https://doi.org/10.1016/S0012-821X(00)00219-3.

Elliott, T., 2004, Tracers of the Slab, *in* Eiler, J., ed., Inside the Subduction Factory: American Geophysical Union, Geophysical Monograph Series, v. 138, p. 23–45, https://doi.org/10.1029/138GM03.

Endo, S., Mizukami, T., Wallis, S.R., Tamura, A., and Arai, S., 2015, Orthopyroxene-rich rocks from the Sanbagawa Belt (SW Japan): Fluid-rock interaction in the forearc slab-mantle wedge interface: Journal of Petrology, v. 56, p. 1113–1137, https://doi.org/10.1093/petrology/egv031.

Engi, M., and Lindsley, D.H., 1980, Stability of titanian clinohumite: Experiments and thermodynamic analysis: Contributions to Mineralogy and Petrology, v. 72, p. 415–424, https://doi.org/10.1007/BF00371348.

Evans, B.W., and Trommsdorff, V., 1978, Petrogenesis of garnet lherzo-lite, Cima di Gagnone, Lepontine Alps: Earth and Planetary Science Letters, v. 40, p. 333–348, https://doi.org/10.1016/0012-821X(78)90158-9.

Evans, B.W., and Trommsdorff, V., 1983, Fluorine hydroxyl titanian clinohumite in Alpine recrystallized garnet peridotite: Compositional controls and petrologic significance: American Journal of Science, v. 283, p. 355–369.

Evans, K.A., 2006, Redox decoupling and redox budgets: Conceptual tools for the study of earth systems: Geology, v. 34, p. 489–492, https://doi.org/10.1130/G22390.1.

Evans, K.A., 2012, The redox budget of subduction zones: Earth-Science Reviews, v. 113, p. 11–32, https://doi.org/10.1016/j.earscirev.2012.03.003.

Evans, K.A., O'Neill, H.S.C., and Mavrogenes, J.A., 2008, Sulphur solubility and sulphide immiscibility in silicate melts as a function of the concentration of manganese, nickel, tungsten and copper at 1 atm and 1400 °C: Chemical Geology, v. 255, no. 1–2, p. 236–249, https://doi.org/10.1016/j.chemgeo.2008.06.042.

Faccenda, M., Gerya, T.V., and Burlini, L., 2009, Deep slab hydration induced by bending-related variations in tectonic pressure: Nature Geoscience, v. 2, p. 790–793, https://doi.org/10.1038/ngeo656.

Ferrando, S., 2012, Mg-metasomatism of metagranitoids from the Alps: Genesis and possible tectonic scenarios: Terra Nova, v. 24, no. 6, p. 423–436, https://doi.org/10.1111/j.1365-3121.2012.01078.x.

Ferrando, S., Frezzotti, M.L., Petrelli, M., and Compagnoni, R., 2009, Metasomatism of continental crust during subduction: The UHP whiteschists from the Southern Dora-Maira Massif (Italian Western Alps): Journal of Metamorphic Geology, v. 27, p. 739–756, https://doi.org/10.1111/j.1525-1314.2009.00837.x.

Ferrando, S., Groppo, C., Frezzotti, M.L., Castelli, D., and Proyer, A., 2017, Dissolving dolomite in a stable UHP mineral assemblage: Evidence from Cal-Dol marbles of the Dora-Maira Massif (Italian Western Alps): The American Mineralogist, v. 102, p. 42–60, https://doi.org/10.2138/am-2017-5761.

Foley, S.F., 2011, A reappraisal of redox melting in the Earth's mantle as a function of tectonic setting and time: Journal of Petrology, v. 52, p. 1363–1391, https://doi.org/10.1093/petrology/egq061.

Frezzotti, M.L., and Ferrando, S., 2015, The chemical behavior of fluids released during deep subduction based on fluid inclusions: The American Mineralogist, v. 100, p. 352–377, https://doi.org/10.2138/am-2015-4933.

Frezzotti, M.L., Selverstone, J., Sharp, Z.D., and Compagnoni, R., 2011, Carbonate dissolution during subduction revealed by diamond-bearing rocks from the Alps: Nature Geoscience, v. 4, p. 703–706, https://doi.org/10.1038/ngeo1246.

Frezzotti, M.-L., Huizenga, J.-M., Compagnoni, R., and Selverstone, J., 2014, Diamond formation by carbon saturation in C-O-H fluids during cold subduction of oceanic lithosphere: Geochimica et Cosmochimica Acta, v. 143, p. 68–86, https://doi.org/10.1016/j.gca.2013.12.022.

Frost, B.R., 1991, Introduction to oxygen fugacity and its petrologic importance, *in* Lindsley, D.H., ed., Oxide Minerals: Petrologic and Magnetic Significance: Mineralogical Society of America, Reviews in Mineralogy, v. 25, p. 1–9.

Downloaded from http://pubs.geoscienceworld.org/gsa/geosphere/article-pdf/14/6/2311/4578874/2311.pdf
by guest

Frost, D.J., and McCammon, C.A., 2008, The Redox State of Earth's Mantle: Annual Review of Earth and Planetary Sciences, v. 36, p. 389–420, https://doi.org/10.1146/annurev.earth.36.031207.124322.

Fu, B., Touret, J.L.R., and Zheng, Y.F., 2003, Remnants of premetamorphic fluid and oxygen isotopic signatures in eclogites and garnet clinopyroxenite from the Dabie-Sulu terranes, eastern China: Journal of Metamorphic Geology, v. 21, p. 561–578, https://doi.org/10.1046/j.1525-1314.2003.00464.x.

Fumagalli, P., and Poli, S., 2005, Experimentally determined phase relations in hydrous peridotites to 6.5 GPa and their consequences on the dynamics of subduction zones: Journal of Petrology, v. 46, p. 555–578, https://doi.org/10.1093/petrology/egh088.

Gao, X.Y., Zheng, Y.F., and Chen, Y.X., 2012, Dehydration melting of ultrahigh-pressure eclogite in the Dabie orogen: Evidence from multiphase solid inclusions in garnet: Journal of Metamorphic Geology, v. 30, p. 193–212, https://doi.org/10.1111/j.1525-1314.2011.00962.x.

Gao, X.Y., Zheng, Y.F., Chen, Y.X., and Hu, Z., 2013, Trace element composition of continentally subducted slab-derived melt: Insight from multiphase solid inclusions in ultrahigh-pressure eclogite in the Dabie orogen: Journal of Metamorphic Geology, v. 31, p. 453–468, https://doi.org/10.1111/jmg.12029.

Gerya, T.V., Stöckhert, B., and Perchuk, A.L., 2002, Exhumation of high-pressure metamorphic rocks in a subduction channel: A numerical simulation: Tectonics, v. 21, https://doi.org/10.1029/2002TC001406.

Grützner, T., Klemme, S., Rohrbach, A., Gervasoni, F., and Berndt, J., 2017, The role of F-clinohumite in volatile recycling processes in subduction zones: Geology, v. 45, p. 443–446, https://doi.org/10.1130/G38788.1.

Gudmundsson, G., and Wood, B.J., 1995, Experimental tests of garnet peridotite oxygen barometry: Contributions to Mineralogy and Petrology, v. 119, p. 56–67, https://doi.org/10.1007/BF00310717.

Guillot, S., Hattori, K.H., De Sigoyer, J., Nägler, T., and Auzende, A.L., 2001, Evidence of hydration of the mantle wedge and its role in the exhumation of eclogites: Earth and Planetary Science Letters, v. 193, p. 115–127, https://doi.org/10.1016/S0012-821X(01)00490-3.

Hack, A.C., and Thompson, A.B., 2011, Density and viscosity of hydrous magmas and related fluids and their role in subduction zone processes: Journal of Petrology, v. 52, p. 1333–1362, https://doi.org/10.1093/petrology/egq048.

Harvey, J., Garrido, C.J., Savov, I., Agostini, S., Padrón-Navarta, J.A., Marchesi, C., Sanchez-Vizcaino, V.L., and Gómez-Pugnaire, M.T., 2014, 11B-rich fluids in subduction zones: The role of antigorite dehydration in subducting slabs and boron isotope heterogeneity in the mantle: Chemical Geology, v. 376, p. 20–30, https://doi.org/10.1016/j.chemgeo.2014.03.015.

Hattori, K.H., and Guillot, S., 2003, Volcanic fronts form as a consequence of serpentinite dehydration in the forearc mantle wedge: Geology, v. 31, p. 525–528, https://doi.org/10.1130/0091-7613(2003)031<0525:VFFAAC>2.0.CO;2.

Hattori, K.H., and Guillot, S., 2007, Geochemical character of serpentinites associated with high- to ultrahigh-pressure metamorphic rocks in the Alps, Cuba, and the Himalayas: Recycling of elements in subduction zones: Geochemistry, Geophysics, Geosystems, v. 8, https://doi.org/10.1029/2007GC001594.

Hermann, J., 2002, Experimental constraints on phase relations in subducted continental crust: Contributions to Mineralogy and Petrology, v. 143, p. 219–235, https://doi.org/10.1007/s00410-001-0336-3.

Hermann, J., and Rubatto, D., 2009, Accessory phase control on the trace element signature of sediment melts in subduction zones: Chemical Geology, v. 265, p. 512–526, https://doi.org/10.1016/j.chemgeo.2009.05.018.

Hermann, J., and Rubatto, D., 2014, Subduction of Continental Crust to Mantle Depth: Geochemistry of Ultrahigh-Pressure Rocks: Treatise on Geochemistry (second edition), v. 4, p. 309–340, https://doi.org/10.1016/B978-0-08-095975-7.00309-0.

Hermann, J., and Spandler, C.J., 2007, Sediment melts at sub-arc depths: An experimental study: Journal of Petrology, v. 49, p. 717–740, https://doi.org/10.1093/petrology/egm073.

Hermann, J., Spandler, C., Hack, A., and Korsakov, A., 2006, Aqueous fluids and hydrous melts in high-pressure and ultra-high pressure rocks: Implications for element transfer in subduction zones: Lithos, v. 92, p. 399–417, https://doi.org/10.1016/j.lithos.2006.03.055.

Hermann, J., Fitz Gerald, J.D., Malaspina, N., Berry, A.J., and Scambelluri, M., 2007, OH-bearing planar defects in olivine produced by the breakdown of Ti-rich humite minerals from Dabie Shan (China): Contributions to Mineralogy and Petrology, v. 153, https://doi.org/10.1007/s00410-006-0155-7.

Hermann, J., Zheng, Y.-F., and Rubatto, D., 2013, Deep fluids in subducted continental crust: Elements, v. 9, p. 281–287, https://doi.org/10.2113/gselements.9.4.281.

Ishii, T., Robinson, P.T., Maekawa, H., and Fiske, R., 1992, Petrological studies of peridotites from diapiric serpentinite seamounts in the Izu-Ogasawara-Mariana Forearc, Leg 125: Proceedings of the Ocean Drilling Program, Scientific Results, v.125, p. 445–485, https://doi.org/10.2973/odp.proc.sr.125.129.1992.

Jahn, B., Fan, Q., Yang, J.-J., and Henin, O., 2003, Petrogenesis of the Maowu pyroxenite-eclogite body from the UHP metamorphic terrane of Dabieshan: Chemical and isotopic constraints: Lithos, v. 70, p. 243–267, https://doi.org/10.1016/S0024-4937(03)00101-4.

John, T., Scherer, E.E., Schenk, V., Herms, P., Halama, R., and Garbe-Schönberg, D., 2010, Subducted seamounts in an eclogite-facies ophiolite sequence: The Andean Raspas Complex, SW Ecuador: Contributions to Mineralogy and Petrology, v. 159, no. 2, p. 265–284, https://doi.org/10.1007/s00410-009-0427-0.

John, T., Scambelluri, M., Frische, M., Barnes, J.D., and Bach, W., 2011, Dehydration of subducting serpentinite: Implications for halogen mobility in subduction zones and the deep halogen cycle: Earth and Planetary Science Letters, v. 308, p. 65–76, https://doi.org/10.1016/j.epsl.2011.05.038.

Kelley, K.A., and Cottrell, E., 2009, Water and the oxidation state of subduction zone magmas: Science, v. 325, p. 605–607, https://doi.org/10.1126/science.1174156.

Kelley, K.A., Plank, T., Ludden, J., and Staudigel, H., 2003, Composition of altered oceanic crust at ODP Sites 801 and 1149: Geochemistry, Geophysics, Geosystems, v. 4, https://doi.org/10.1029/2002GC000435.

Kendrick, M.A., Scambelluri, M., Honda, M., and Phillips, D., 2011, High abundances of noble gas and chlorine delivered to the mantle by serpentinite subduction: Nature Geoscience, v. 4, p. 807–812, https://doi.org/10.1038/ngeo1270.

Kendrick, M.A., Honda, M., Pettke, T., Scambelluri, M., Phillips, D., and Giuliani, A., 2013, Subduction zone fluxes of halogens and noble gases in seafloor and forearc serpentinites: Earth and Planetary Science Letters, v. 365, p. 86–96, https://doi.org/10.1016/j.epsl.2013.01.006.

Kendrick, M.A., Hémond, C., Kamenetsky, V.S., Danyushevsky, L., Devey, C.W., Rodemann, T., Jackson, M.G., and Perfit, M.R., 2017, Seawater cycled throughout Earth's mantle in partially serpentinized lithosphere: Nature Geoscience, v. 10, p. 222–228, https://doi.org/10.1038/ngeo2902.

Kessel, R., Schmidt, M.W., Ulmer, P., and Pettke, T., 2005a, Trace element signature of subduction-zone fluids, melts and supercritical liquids at 120–180 km depth: Nature, v. 437, p. 724–727, https://doi.org/10.1038/nature03971.

Kessel, R., Ulmer, P., Pettke, T., Schmidt, M.W., and Thompson, A.B., 2005b, The water-basalt system at 4 to 6 GPa: Phase relations and second critical endpoint in a K-free eclogite at 700 to 1400 °C: Earth and Planetary Science Letters, v. 237, p. 873–892, https://doi.org/10.1016/j.epsl.2005.06.018.

Klein, E.M., 2003, Geochemistry of the Igneous Oceanic Crust: Treatise on Geochemistry, v. 3, p. 433–463, https://doi.org/10.1016/B0-08-043751-6/03030-9.

Klimm, K., Blundy, J.D., and Green, T.H., 2008, Trace element partitioning and accessory phase saturation during H_2O-saturated melting of basalt with implications for subduction zone chemical fluxes: Journal of Petrology, v. 44, no. 3, p. 523–553, https://doi.org/10.1093/petrology/egn001.

Kodolányi, J., and Pettke, T., 2011, Loss of trace elements from serpentinites during fluid-assisted transformation of chrysotile to antigorite—An example from Guatemala: Chemical Geology, v. 284, p. 351–362, https://doi.org/10.1016/j.chemgeo.2011.03.016.

Kodolányi, J., Pettke, T., Spandler, C., Kamber, B.S., and Ling, K.G., 2012, Geochemistry of ocean floor and fore-arc serpentinites: Constraints on the ultramafic input to subduction zones: Journal of Petrology, v. 53, p. 235–270, https://doi.org/10.1093/petrology/egr058.

Korzhinskii, D.S., 1959, Physicochemical Basis of the Analysis of the Paragenesis of Minerals: New York, Consultants Bureau, 142 p.

Korzhinskii, D.S., 1965, The theory of systems with perfectly mobile components and processes of mineral formation: American Journal of Science, v. 263, p. 193–205, https://doi.org/10.2475/ajs.263.3.193.

Lafay, R., Deschamps, F., Schwartz, S., Guillot, S., Godard, M., Debret, B., and Nicollet, C., 2013, High-pressure serpentinites, a trap-and-release system controlled by metamorphic conditions: Example from the Piedmont zone of the western Alps: Chemical Geology, v. 343, p. 38–54, https://doi.org/10.1016/j.chemgeo.2013.02.008.

Downloaded from http://pubs.geoscienceworld.org/gsa/geosphere/article-pdf/14/6/2311/4578874/2311.pdf
by guest

Lafay, R., Baumgartner, L.P., Stephane, S., Suzanne, P., German, M.H., and Torsten, V., 2017, Petrologic and stable isotopic studies of a fossil hydrothermal system in ultramafic environment (Chenaillet ophicalcites, Western Alps, France): Processes of carbonate cementation: Lithos, v. 294–295, p. 319–338, https://doi.org/10.1016/j.lithos.2017.10.006.

Lagabrielle, Y., Karpoff, A.-M., and Cotten, J., 1992, Mineralogical and Geochemical Analyses of Sedimentary Serpentinites from Conical Seamount (Hole 788A): Implication for the Evolution of Serpentine Seamounts, *in* Proceedings of the Ocean Drilling Program, Scientific Results, v. 125, p. 325–342, https://doi.org/10.2973/odp.proc.sr.125.175.1992.

Lee, C.-T., Leeman, W.P., Canil, D., and A Li, Z.X., 2005, Similar V/Sc systematics in MORB and arc basalts: Implications for the oxygen fugacities of their mantle source regions: Journal of Petrology, v. 46, p. 2313–2336, https://doi.org/10.1093/petrology/egi056.

Li, J.-L., Gao, J., Klemd, R., John, T., and Wang, X.-S., 2016, Redox processes in subducting oceanic crust recorded by sulfide-bearing high-pressure rocks and veins (SW Tianshan, China): Contributions to Mineralogy and Petrology, v. 171, p. 72, https://doi.org/10.1007/s00410-016-1284-2.

Li, Y.H., 1991, Distribution patterns of the elements in the ocean: A synthesis: Geochimica et Cosmochimica Acta, v. 55, p. 3223–3240, https://doi.org/10.1016/0016-7037(91)90485-N.

López Sánchez-Vizcaíno, V., Trommsdorff, V., Gómez-Pugnaire, M.T., Garrido, C.J., Müntener, O., and Connolly, J.A.D., 2005, Petrology of titanian clinohumite and olivine at the high-pressure breakdown of antigorite serpentinite to chlorite harzburgite (Almirez Massif, S. Spain): Contributions to Mineralogy and Petrology, v. 149, p. 627–646, https://doi.org/10.1007/s00410-005-0678-3.

Lundin, E.R., and Doré, A.G., 2011, Hyperextension, serpentinization, and weakening: A new paradigm for rifted margin compressional deformation: Geology, v. 39, p. 347–350, https://doi.org/10.1130/G31499.1.

Luth, R.W., Virgo, D., Boyd, F.R., and Wood, B.J., 1990, Ferric iron in mantle-derived garnets Implications for thermobarometry and for the oxidation state of the mantle: Contributions to Mineralogy and Petrology, v. 104, p. 56–72, https://doi.org/10.1007/BF00310646.

Malaspina, N., and Tumiati, S., 2012, The role of C-O-H and oxygen fugacity in subduction-zone garnet peridotites: European Journal of Mineralogy, v. 24, p. 607–618, https://doi.org/10.1127/0935-1221/2012/0024-2213.

Malaspina, N., Hermann, J., Scambelluri, M., and Compagnoni, R., 2006a, Multistage metasomatism in ultrahigh-pressure mafic rocks from the North Dabie Complex (China): Lithos, v. 90, p. 19–42, https://doi.org/10.1016/j.lithos.2006.01.002.

Malaspina, N., Hermann, J., Scambelluri, M., and Compagnoni, R., 2006b, Polyphase inclusions in garnet-orthopyroxenite (Dabie Shan, China) as monitors for metasomatism and fluid-related trace element transfer in subduction zone peridotite: Earth and Planetary Science Letters, v. 249, p. 173–187, https://doi.org/10.1016/j.epsl.2006.07.017.

Malaspina, N., Hermann, J., and Scambelluri, M., 2009a, Fluid/mineral interaction in UHP garnet peridotite: Lithos, v. 107, p. 38–52, https://doi.org/10.1016/j.lithos.2008.07.006.

Malaspina, N., Poli, S., and Fumagalli, P., 2009b, The oxidation state of metasomatized mantle wedge: Insights from C-O-H-bearing garnet peridotite: Journal of Petrology, v. 50, p. 1533–1552, https://doi.org/10.1093/petrology/egp040.

Malaspina, N., Scambelluri, M., Poli, S., Van Roermund, H.L.M., and Langenhorst, F., 2010, The oxidation state of mantle wedge majoritic garnet websterites metasomatised by C-bearing subduction fluids: Earth and Planetary Science Letters, v. 298, p. 417–426, https://doi.org/10.1016/j.epsl.2010.08.022.

Malaspina, N., Langenhorst, F., Fumagalli, P., Tumiati, S., and Poli, S., 2012, Fe^{3+} distribution between garnet and pyroxenes in mantle wedge carbonate-bearing garnet peridotites (Sulu, China) and implications for their oxidation state: Lithos, v. 146–147, p. 11–17, https://doi.org/10.1016/j.lithos.2012.04.023.

Malaspina, N., Langenhorst, F., Tumiati, S., Campione, M., Frezzotti, M.L., and Poli, S., 2017, The redox budget of crust-derived fluid phases at the slab-mantle interface: Geochimica et Cosmochimica Acta, v. 209, p. 70–84, https://doi.org/10.1016/j.gca.2017.04.004.

Marchesi, C., Garrido, C.J., Godard, M., Proenza, J.A., Gervilla, F., and Blanco-Moreno, J., 2006, Petrogenesis of highly depleted peridotites and gabbroic rocks from the Mayarí-Baracoa Ophiolitic Belt (eastern Cuba): Contributions to Mineralogy and Petrology, v. 151, p. 717–736, https://doi.org/10.1007/s00410-006-0089-0.

Marchesi, C., Garrido, C.J., Godard, M., Belley, F., and Ferré, E., 2009, Migration and accumulation of ultra-depleted subduction-related melts in the Massif du Sud ophiolite (New Caledonia): Chemical Geology, v. 266, p. 171–186, https://doi.org/10.1016/j.chemgeo.2009.06.004.

Marchesi, C., Garrido, C.J., Padrón-Navarta, J.A., López Sánchez-Vizcaíno, V., and Gómez-Pugnaire, M.T., 2013, Element mobility from seafloor serpentinization to high-pressure dehydration of antigorite in subducted serpentinite: Insights from the Cerro del Almirez ultramafic massif (southern Spain): Lithos, v. 178, p. 128–142, https://doi.org/10.1016/j.lithos.2012.11.025.

Marschall, H.R., and Schumacher, J.C., 2012, Arc magmas sourced from mélange diapirs in subduction zones: Nature Geoscience, v. 5, p. 862–867, https://doi.org/10.1038/ngeo1634.

Marschall, H.R., Ludwig, T., Altherr, R., Kalt, A., and Tonarini, S., 2006, Syros metasomatic tourmaline: Evidence for very high-δ11B fluids in subduction zones: Journal of Petrology, v. 47, p. 1915–1942, https://doi.org/10.1093/petrology/egl031.

Martin, L.A.J., Hermann, J., Gauthiez-Putallaz, L., Whitney, D.L., Vitale Brovarone, A., Fornash, K.F., and Evans, N.J., 2014, Lawsonite geochemistry and stability—Implication for trace element and water cycles in subduction zones: Journal of Metamorphic Geology, v. 32, no. 5, p. 455–478, https://doi.org/10.1111/jmg.12093.

Mattinson, C.G., Zhang, R.Y., Tsujimori, T., and Liou, J.G., 2004, Epidote-rich talc-kyanite-phengite eclogites, Sulu terrane, eastern China: P-T-fo2 estimates and the significance of the epidote-talc assemblage in eclogite: The American Mineralogist, v. 89, p. 1772–1783, https://doi.org/10.2138/am-2004-11-1224.

McArthur, J.M., Howarth, R.J., and Bailey, T.R., 2001, Strontium isotope stratigraphy: LOWESS version 3: Best fit to the marine Sr-isotope curve for 0–509 Ma and accompanying look-up table for deriving numerical age: The Journal of Geology, v. 109, p. 155–170, https://doi.org/10.1086/319243.

McDonough, W.F., and Sun, S.S., 1995, The composition of the Earth: Chemical Geology, v. 120, p. 223–253, https://doi.org/10.1016/0009-2541(94)00140-4.

Mével, C., 2003, Serpentinization of abyssal peridotites at mid-ocean ridges: Comptes Rendus Geoscience, v. 335, p. 825–852, https://doi.org/10.1016/j.crte.2003.08.006.

Mohn, G., Manatschal, G., Beltrando, M., and Haupert, I., 2014, The role of rift-inherited hyperextension in Alpine-type orogens: Terra Nova, v. 26, p. 347–353, https://doi.org/10.1111/ter.12104.

Moore, J.C., and Vrolijk, P., 1992, Correction to "Fluids in accretionary prisms": Reviews of Geophysics, v. 30, p. 113–135, https://doi.org/10.1029/92RG02601.

Morishita, T., Hara, K., Nakamura, K., Sawaguchi, T., Tamura, A., Arai, S., Okino, K., Takai, K., and Kumagai, H., 2009, Igneous, alteration and exhumation processes recorded in abyssal peridotites and related fault rocks from an oceanic core complex along the Central Indian Ridge: Journal of Petrology, v. 50, p. 1299–1325, https://doi.org/10.1093/petrology/egp025.

Newton, R.C., and Manning, C.E., 2002, Solubility of enstatite + forsterite in H2O at deep crust/upper mantle conditions: 4 to 15 kbar and 700 to 900 ° C: Geochimica et Cosmochimica Acta, v. 66, p. 4165–4176, https://doi.org/10.1016/S0016-7037(02)00998-5.

Newton, R.C., and Manning, C.E., 2005, Solubility of anhydrite, $CaSO_4$, in NaCl-H_2O solutions at high pressures and temperatures: Applications to fluid-rock interaction: Journal of Petrology, v. 46, p. 701–716, https://doi.org/10.1093/petrology/egh094.

Nichols, G.T., Wyllie, P.J., and Stern, C.R., 1994, Subduction zone melting of pelagic sediments constrained by melting experiments: Nature, v. 371, p. 785–788, https://doi.org/10.1038/371785a0.

Nielsen, S.G., and Marschall, H.R., 2017, Geochemical evidence for mélange melting in global arcs: Science Advances, v. 3, e1602402, https://doi.org/10.1126/sciadv.1602402.

Nimis, P., and Morten, L., 2000, P-T evolution of "crustal" garnet peridotites and included pyroxenites from Nonsberg area (upper Austroalpine), NE Italy: From the wedge to the slab: Journal of Geodynamics, v. 30, p. 93–115, https://doi.org/10.1016/S0264-3707(99)00029-0.

Niu, Y., 2004, Bulk-rock major and trace element compositions of abyssal peridotites: Implications for mantle melting, melt extraction and post-melting processes beneath mid-ocean ridges: Journal of Petrology, v. 45, p. 2423–2458, https://doi.org/10.1093/petrology/egh068.

O'Hanley, D.S., 1992, Solution to the volume problem in serpentinization: Geology, v. 20, p. 705–708, https://doi.org/10.1130/0091-7613(1992)020<0705:STTVPI>2.3.CO;2.

Onishi, H., and Sandell, E.B., 1955, Geochemistry of arsenic: Geochimica et Cosmochimica Acta, v. 7, p. 1–33, https://doi.org/10.1016/0016-7037(55)90042-9.

Padrón-Navarta, J.A., Sánchez-Vizcaíno, V.L., Hermann, J., Connolly, J.A.D., Garrido, C.J., Gómez-Pugnaire, M.T., and Marchesi, C., 2013, Tschermak's substitution in antigorite and consequences for phase relations and water liberation in high-grade serpentinites: Lithos, https://doi.org/10.1016/j.lithos.2013.02.001.

Parkinson, I.J., and Arculus, R.J., 1999, The redox state of subduction zones: Insights from arc-peridotites: Chemical Geology, v. 160, p. 409–423, https://doi.org/10.1016/S0009-2541(99)00110-2.

Downloaded from http://pubs.geoscienceworld.org/gsa/geosphere/article-pdf/14/6/2311/4578874/2311.pdf
by guest

Parkinson, I.J., and Pearce, J.A., 1998, Peridotites from the Izu-Bonin-Mariana forearc (ODP Leg 125): Evidence for mantle melting and melt-mantle interaction in a supra-subduction zone setting: Journal of Petrology, v. 39, p. 1577–1618, https://doi.org/10.1093/petroj/39.9.1577.

Paulick, H., Bach, W., Godard, M., De Hoog, J.C.M., Suhr, G., and Harvey, J., 2006, Geochemistry of abyssal peridotites (Mid-Atlantic Ridge, 15°20′N, ODP Leg 209): Implications for fluid/rock interaction in slow spreading environments: Chemical Geology, v. 234, p. 179–210, https://doi.org/10.1016/j.chemgeo.2006.04.011.

Peacock, S.M., 1993, The importance of blueschist → eclogite dehydration reactions in subducting oceanic crust: Geological Society of America Bulletin, v. 105, p. 684–694, https://doi.org/10.1130/0016-7606(1993)105<0684:TIOBED>2.3.CO;2.

Peacock, S.M., 1996, Thermal and petrologic structure of subduction zones *in* Bebout, G.E., et al., eds., Subduction: Top to Bottom: American Geophysical Union, Geophysical Monograph Series, v. 96, p. 119–133, https://doi.org/10.1029/GM096p0019.

Pearce, J.A., Barker, P.F., Edwards, S.J., Parkinson, I.J., and Leat, P.T., 2000, Geochemistry and tectonic significance of peridotites from the South Sandwich arc-basin system, South Atlantic: Contributions to Mineralogy and Petrology, v. 139, p. 36–53, https://doi.org/10.1007/s004100050572.

Pearce, J.A., Stern, R.J., Bloomer, S.H., and Fryer, P., 2005, Geochemical mapping of the Mariana arc-basin system: Implications for the nature and distribution of subduction components: Geochemistry, Geophysics, Geosystems, v. 6, https://doi.org/10.1029/2004GC000895.

Perfit, M.R., and Chadwick, W.W., 1998, Magmatism at mid-ocean ridges: Constraints from volcanological and geochemical investigations, *in* Buck, W.R., Delaney, P.T., Karson, J.A., and Lagabrielle, Y., eds., Faulting and Magmatism at Mid-Ocean Ridges: American Geophysical Union, Geophysical Monograph Series, v. 106, https://doi.org/10.1029/GM106p0059.

Peron-Pinvidic, G., and Manatschal, G., 2010, From microcontinents to extensional allochthons: Witnesses of how continents rift and break apart?: Petroleum Geoscience, v. 16, p. 189–197, https://doi.org/10.1144/1354-079309-903.

Peslier, A.H., Luhr, J.F., and Post, J., 2002, Low water contents in pyroxenes from spinel-peridotites of the oxidized, sub-arc mantle wedge: Earth and Planetary Science Letters, v. 201, p. 69–86, https://doi.org/10.1016/S0012-821X(02)00663-5.

Peters, D., Bretscher, A., John, T., Scambelluri, M., and Pettke, T., 2017, Fluid-mobile elements in serpentinites: Constraints on serpentinisation environments and element cycling in subduction zones: Chemical Geology, v. 466, p. 654–666, https://doi.org/10.1016/j.chemgeo.2017.07.017.

Philippot, P., and Selverstone, J., 1991, Trace-element-rich brines in eclogitic veins: Implications for fluid composition and transport during subduction: Contributions to Mineralogy and Petrology, v. 106, p. 417–430, https://doi.org/10.1007/BF00321985.

Philippot, P., Chevallier, P., Chopin, C., and Dubessy, J., 1995, Fluid composition and evolution in coesite-bearing rocks (Dora-Maira massif, Western Alps): Implications for element recycling during subduction: Contributions to Mineralogy and Petrology, v. 121, https://doi.org/10.1007/s004100050088.

Pirard, C., and Hermann, J., 2015, Focused fluid transfer through the mantle above subduction zones: Geology, v. 43, no. 10, p. 915–918, https://doi.org/10.1130/G37026.1.

Plank, T., 2014, The Chemical Composition of Subducting Sediments: Reference Module in Earth Systems and Environmental Sciences: Treatise on Geochemistry (second edition), v. 4, p. 607–629, https://doi.org/10.1016/B978-0-08-095975-7.00319-3.

Plank, T., and Langmuir, C.H., 1998, The chemical composition of subducting sediment and its consequences for the crust and mantle: Chemical Geology, v. 145, p. 325–394, https://doi.org/10.1016/S0009-2541(97)00150-2.

Plank, T., and Ludden, J.N., 1992, Geochemistry of Sediments in the Argo Abyssal Plain at Site 765: A Continental Margin Reference Section for Sediment Recycling in Subduction Zones, *in* Gradstein, F.M., Ludden, J.N., et al., eds., Proceedings of the Ocean Drilling Program, Scientific Results, v. 123, p. 167–189, https://doi.org/10.2973/odp.proc.sr.123.158.1992.

Poli, S., and Schmidt, M.W., 2002, Petrology of Subducted Slabs: Annual Review of Earth and Planetary Sciences, v. 30, p. 207–235, https://doi.org/10.1146/annurev.earth.30.091201.140550.

Ranero, C.R., Phipps Morgan, J., McIntosh, K., and Relchert, C., 2003, Bending-related faulting and mantle serpentinization at the Middle America trench: Nature, v. 425, p. 367–373, https://doi.org/10.1038/nature01961.

Ranero, C.R., Villaseñor, A., Morgan, J.P., and Weinrebe, W., 2005, Relationship between bend-faulting at trenches and intermediate-depth seismicity: Geochemistry, Geophysics, Geosystems, v. 6, no. 12, https://doi.org/10.1029/2005GC000997.

Rehkämper, M., and Hofmann, A.W., 1997, Recycled ocean crust and sediment in Indian Ocean MORB: Earth and Planetary Science Letters, v. 147, no. 1–4, p. 93–106, https://doi.org/10.1016/S0012-821X(97)00009-5.

Rielli, A., Tomkins, A.G., Nebel, O., Brugger, J., Etschmann, B., Zhong, R., Yaxley, G.M., and Paterson, D., 2017, Evidence of sub-arc mantle oxidation by sulphur and carbon: Geochemical Perspectives Letters, p. 124–132, https://doi.org/10.7185/geochemlet.1713.

Rohrbach, A., Schuth, S., Ballhaus, C., Münker, C., Matveev, S., and Qopoto, C., 2005, Petrological constraints on the origin of arc picrites, New Georgia Group, Solomon Islands: Contributions to Mineralogy and Petrology, v. 149, p. 685–698, https://doi.org/10.1007/s00410-005-0675-6.

Rohrbach, A., Ballhaus, C., Golla-Schindler, U., Ulmer, P., Kamenetsky, V.S., and Kuzmin, D.V., 2007, Metal saturation in the upper mantle: Nature, v. 449, p. 456–458, https://doi.org/10.1038/nature06183.

Rohrbach, A., Ballhaus, C., Ulmer, P., Golla-Schindler, U., and Schonbohm, D., 2011, Experimental evidence for a reduced metal-saturated upper mantle: Journal of Petrology, v. 52, p. 717–731, https://doi.org/10.1093/petrology/egq101.

Rubatto, D., and Hermann, J., 2003, Zircon formation during fluid circulation in eclogites (Monviso, Western Alps): Implications for Zr and Hf budget in subduction zones: Geochimica et Cosmochimica Acta, v. 67, p. 2173–2187, https://doi.org/10.1016/S0016-7037(02)01321-2.

Rudnick, R.L., and Gao, S., 2014, Composition of the Continental Crust: Treatise on Geochemistry (second edition), v. 4, p. 1–51, https://doi.org/10.1016/B978-0-08-095975-7.00301-6.

Rüpke, L.H., Morgan, J.P., Hort, M., and Connolly, J.A.D., 2004, Serpentine and the subduction zone water cycle: Earth and Planetary Science Letters, v. 223, p. 17–34, https://doi.org/10.1016/j.epsl.2004.04.018.

Sadofsky, S.J., and Bebout, G.E., 2003, Record of forearc devolatilization in low-T, high-P/T metasedimentary suites: Significance for models of convergent margin chemical cycling: Geochemistry, Geophysics, Geosystems, v. 4, no. 4, https://doi.org/10.1029/2002GC000412.

Salters, V.J.M., and Stracke, A., 2004, Composition of the depleted mantle: Geochemistry, Geophysics, Geosystems, v. 5, no. 5, https://doi.org/10.1029/2003GC000597.

Sapienza, G.T., Scambelluri, M., and Braga, R., 2009, Dolomite-bearing orogenic garnet peridotites witness fluid-mediated carbon recycling in a mantle wedge (Ulten Zone, Eastern Alps, Italy): Contributions to Mineralogy and Petrology, v. 158, p. 401–420, https://doi.org/10.1007/s00410-009-0389-2.

Saumur, B.M., Hattori, K.H., and Guillot, S., 2010, Contrasting origins of serpentinites in a subduction complex, northern Dominican Republic: Bulletin of the Geological Society of America, v. 122, p. 292–304, https://doi.org/10.1130/B26530.1.

Savov, I.P., Ryan, J.G., D'Antonio, M., Kelley, K., and Mattie, P., 2005, Geochemistry of serpentinized peridotites from the Mariana Forearc Conical Seamount, ODP Leg 125: Implications for the elemental recycling at subduction zones: Geochemistry, Geophysics, Geosystems, v. 6, no. 4, https://doi.org/10.1029/2004GC000777.

Savov, I.P., Ryan, J.G., D'Antonio, M., and Fryer, P., 2007, Shallow slab fluid release across and along the Mariana arc-basin system: Insights from geochemistry of serpentinized peridotites from the Mariana fore arc: Journal of Geophysical Research. Solid Earth, v. 112, B9, https://doi.org/10.1029/2006JB004749.

Scambelluri, M., and Philippot, P., 2001, Deep fluids in subduction zones: Lithos, v. 55, p. 213–227, https://doi.org/10.1016/S0024-4937(00)00046-3.

Scambelluri, M., and Tonarini, S., 2012, Boron isotope evidence for shallow fluid transfer across subduction zones by serpentinized mantle: Geology, v. 40, p. 907–910, https://doi.org/10.1130/G33233.1.

Scambelluri, M., Müntener, O., Hermann, J., Piccardo, G.B., and Trommsdorff, V., 1995, Subduction of water into the mantle: history of an Alpine peridotite: Geology, v. 23, p. 459–462, https://doi.org/10.1130/0091-7613.

Scambelluri, M., Bottazzi, P., Trommsdor, V., Vannucci, R., Hermann, J., and Go, M.T., 2001, Incompatible element-rich fluids released by antigorite breakdown in deeply subducted mantle: Earth and Planetary Science Letters, v. 192, p. 457–470, https://doi.org/10.1016/S0012-821X(01)00457-5.

Scambelluri, M., Fiebig, J., Malaspina, N., Müntener, O., and Pettke, T., 2004, Serpentinite Subduction: Implications for Fluid Processes and Trace-Element Recycling: International Geology Review, v. 46, p. 595–613, https://doi.org/10.2747/0020-6814.46.7.595.

Scambelluri, M., Hermann, J., Morten, L., and Rampone, E., 2006, Melt- versus fluid-induced metasomatism in spinel to garnet wedge peridotites (Ulten Zone, Eastern Italian Alps): Clues

Downloaded from http://pubs.geoscienceworld.org/gsa/geosphere/article-pdf/14/6/2311/4578874/2311.pdf
by guest

from trace element and Li abundances: Contributions to Mineralogy and Petrology, v. 151, p. 372–394, https://doi.org/10.1007/s00410-006-0064-9.
Scambelluri, M., Malaspina, N., and Hermann, J., 2007, Subduction fluids and their interaction with the mantle wedge: A perspective from the study of high-pressure ultramafic rocks: Periodico di Mineralogia, v. 76, p. 253–265, https://doi.org/10.2451/2007PM0028.
Scambelluri, M., Pettke, T., and van Roermund, H.L.M., 2008, Majoritic garnets monitor deep subduction fluid flow and mantle dynamics: Geology, v. 36, p. 59, https://doi.org/10.1130/G24056A.1.
Scambelluri, M., Van Roermund, H.L.M., and Pettke, T., 2010, Mantle wedge peridotites: Fossil reservoirs of deep subduction zone processes: Lithos, v. 120, p. 186–201, https://doi.org/10.1016/j.lithos.2010.03.001.
Scambelluri, M., Pettke, T., Rampone, E., Godard, M., and Reusser, E., 2014, Petrology and trace element budgets of high-pressure peridotites indicate subduction dehydration of serpentinized mantle (Cima di Gagnone, Central Alps, Switzerland): Journal of Petrology, v. 55, p. 459–498, https://doi.org/10.1093/petrology/egt068.
Scambelluri, M., Pettke, T., and Cannaò, E., 2015, Fluid-related inclusions in Alpine high-pressure peridotite reveal trace element recycling during subduction-zone dehydration of serpentinized mantle (Cima di Gagnone, Swiss Alps): Earth and Planetary Science Letters, v. 429, p. 45–59, https://doi.org/10.1016/j.epsl.2015.07.060.
Schertl, H.-P., and Schreyer, W., 2008, Geochemistry of coesite-bearing "pyrope quartzite" and related rocks from the Dora-Maira Massif, Western Alps: European Journal of Mineralogy, v. 20, p. 791–809, https://doi.org/10.1127/0935-1221/2008/0020-1862.
Schmidt, M.W., and Poli, S., 1994, The stability of lawsonite and zoisite at high pressures: Experiments in CASH to 92 kbar and implications for the presence of hydrous phases in subducted lithosphere: Earth and Planetary Science Letters, https://doi.org/10.1016/0012-821X(94)00080-8.
Schmidt, M.W., and Poli, S., 2014, Devolatilization during Subduction: Treatise on Geochemistry (second edition), v. 4, https://doi.org/10.1016/B978-0-08-095975-7.00321-1.
Schmidt, M.W., Vielzeuf, D., and Auzanneau, E., 2004, Melting and dissolution of subducting crust at high pressures: The key role of white mica: Earth and Planetary Science Letters, v. 228, p. 65–84, https://doi.org/10.1016/j.epsl.2004.09.020.
Schneider, M.E., and Eggler, D.H., 1986, Fluids in equilibrium with peridotite minerals: Implications for mantle metasomatism: Geochimica et Cosmochimica Acta, v. 50, p. 711–724, https://doi.org/10.1016/0016-7037(86)90347-9.
Schwarzenbach, E.M., Früh-Green, G.L., Bernasconi, S.M., Alt, J.C., and Plas, A., 2013, Serpentinization and carbon sequestration: A study of two ancient peridotite-hosted hydrothermal systems: Chemical Geology, v. 351, p. 115–133, https://doi.org/10.1016/j.chemgeo.2013.05.016.
Smith, D.C., 1984, Coesite in clinopyroxene in the Caledonides and its implications for geodynamics: Nature, v. 310, p. 641–644, https://doi.org/10.1038/310641a0.
Smith, H.J., Spivack, A.J., Staudigel, H., and Hart, S.R., 1995, The boron isotopic composition of altered oceanic crust: Chemical Geology, v. 126, p. 119–135, https://doi.org/10.1016/0009-2541(95)00113-6.
Sobolev, N.V., and Shatsky, V.S., 1990, Diamond inclusions in garnets from metamorphic rocks: A new environment for diamond formation: Nature, v. 343, p. 742–746, https://doi.org/10.1038/343742a0.
Spandler, C., and Pirard, C., 2013, Element recycling from subducting slabs to arc crust: A review: Lithos, v. 170–171, p. 208–223, https://doi.org/10.1016/j.lithos.2013.02.016.
Spandler, C., Hermann, J., Arculus, R., and Mavrogenes, J., 2003, Redistribution of trace elements during prograde metamorphism from lawsonite blueschist to eclogite facies: Implications for deep subduction-zone processes: Contributions to Mineralogy and Petrology, v. 146, p. 205–222, https://doi.org/10.1007/s00410-003-0495-5.
Spandler, C., Hermann, J., Arculus, R., and Mavrogenes, J., 2004, Geochemical heterogeneity and element mobility in deeply subducted oceanic crust: Insights from high-pressure mafic rocks from New Caledonia: Chemical Geology, v. 206, p. 21–42, https://doi.org/10.1016/j.chemgeo.2004.01.006.
Spandler, C., Mavrogenes, J., and Hermann, J., 2007, Experimental constraints on element mobility from subducted sediments using high-P synthetic fluid/melt inclusions: Chemical Geology, v. 239, p. 228–249, https://doi.org/10.1016/j.chemgeo.2006.10.005.
Spandler, C., Pettke, T., and Hermann, J., 2014, Experimental study of trace element release during ultrahigh-pressure serpentinite dehydration: Earth and Planetary Science Letters, v. 391, p. 296–306, https://doi.org/10.1016/j.epsl.2014.02.010.
Spengler, D., Brueckner, H.K., van Roermund, H.L.M., Drury, M.R., and Mason, P.R.D., 2009, Long-lived, cold burial of Baltica to 200 km depth: Earth and Planetary Science Letters, v. 281, p. 27–35, https://doi.org/10.1016/j.epsl.2009.02.001.
Stagno, V., Ojwang, D.O., McCammon, C.A, and Frost, D.J., 2013, The oxidation state of the mantle and the extraction of carbon from Earth's interior: Nature, v. 493, p. 84–88, https://doi.org/10.1038/nature11679.
Stalder, R., and Ulmer, P., 2001, Phase relations of a serpentine composition between 5 and 14 GPa: Significance of clinohumite and phase E as water carriers into the transition zone: Contributions to Mineralogy and Petrology, v. 140, p. 670–679, https://doi.org/10.1007/s004100000208.
Staudigel, H., 2003, Hydrothermal alteration processes in the oceanic crust: Treatise on Geochemistry, v. 3, p. 511–535,https://doi.org/10.1016/B0-08-043751-6/03032-2.
Staudigel, H., Plank, T., White, B., and Schmincke, H.U., 1996, Geochemical fluxes during seafloor alteration of the basaltic upper oceanic crust: DSDP sites 417 and 418, *in* Bebout, G.E., Scholl, D.W., Kirby, S.H., and Platt, J.P., eds., Subduction: Top to Bottom: American Geophysical Union, Geophysical Monograph Series, v. 96, https://doi.org/10.1029/GM096p0019.
Stepanov, A.S., Hermann, J., Korsakov, A.V., and Rubatto, D., 2014, Geochemistry of ultrahigh-pressure anatexis: Fractionation of elements in the Kokchetav gneisses during melting at diamond-facies conditions: Contributions to Mineralogy and Petrology, v. 167, p. 1–25, https://doi.org/10.1007/s00410-014-1002-x.
Stepanov, A.S., Hermann, J., Rubatto, D., Korsakov, A.V., and Danyushevsky, L.V., 2016, Melting history of an ultrahigh-pressure paragneiss revealed by multiphase solid inclusions in garnet, Kokchetav massif, Kazakhstan: Journal of Petrology, v. 57, p. 1531–1554, https://doi.org/10.1093/petrology/egw049.
Stern, R.J., 2002, Subduction zones: Reviews of Geophysics, v. 40, p. 1012, https://doi.org/10.1029/2001RG000108.
Stöckhert, B., Duyster, J., Trepmann, C., Massonne, H., and Sto, B., 2001, Microdiamond daughter crystals precipitated from supercritical COH + silicate fluids included in garnet, Erzgebirge, Germany: Geology, v. 29, p. 391–394, https://doi.org/10.1130/0091-7613(2001)029<0391.
Syracuse, E.M., van Keken, P.E., Abers, G.A., Suetsugu, D., Bina, C., Inoue, T., Wiens, D., and Jellinek, M., 2010, The global range of subduction zone thermal models: Physics of the Earth and Planetary Interiors, v. 183, p. 73–90, https://doi.org/10.1016/j.pepi.2010.02.004.
Tatsumi, Y., 1986, Formation of the volcanic front in subduction zones: Geophysical Research Letters, v. 13, p. 717–720, https://doi.org/10.1029/GL013i008p00717.
Tatsumi, Y., 2005, The subduction factory: How it operates in the evolving Earth: GSA Today, v. 15, no. 7, p. 4–10, https://doi.org/10.1130/1052-5173(2005)015[4:TSFHIO]2.0.CO;2.
Tatsumi, Y., and Eggins, S., 1997, Subduction Zone Magmatism: Surveys in Geophysics: Blackwell Science, 211 p.
Tenthorey, E., and Hermann, J., 2004, Composition of fluids during serpentinite breakdown in subduction zones: Evidence for limited boron mobility: Geology, v. 32, p. 865–868, https://doi.org/10.1130/G20610.1.
Tiepolo, M., Oberti, R., Zanetti, A., Vannucci, R., and Foley, S.F., 2007, Trace-Element Partitioning between Amphibole and Silicate Melt: Reviews in Mineralogy and Geochemistry, v. 67, p. 417–452, https://doi.org/10.2138/rmg.2007.67.11.
Till, C.B., Grove, T.L., and Withers, A.C., 2012, The beginnings of hydrous mantle wedge melting: Contributions to Mineralogy and Petrology, v. 163, p. 669–688, https://doi.org/10.1007/s00410-011-0692-6.
Trommsdorff, V., and Evans, B.W., 1980, Titanian hydroxyl-clinohumite: Formation and breakdown in antigorite rocks (Malenco, Italy): Contributions to Mineralogy and Petrology, v. 72, p. 229–242, https://doi.org/10.1007/BF00376142.
Tsay, A., Zajacz, Z., and Sanchez-Valle, C., 2014, Efficient mobilization and fractionation of rare-earth elements by aqueous fluids upon slab dehydration: Earth and Planetary Science Letters, v. 398, p. 101–112, https://doi.org/10.1016/j.epsl.2014.04.042.
Tsay, A., Zajacz, Z., Ulmer, P., and Sanchez-Valle, C., 2017, Mobility of major and trace elements in the eclogite-fluid system and element fluxes upon slab dehydration: Geochimica et Cosmochimica Acta, v. 198, p. 70–91, https://doi.org/10.1016/j.gca.2016.10.038.
Tumiati, S., Thöni, M., Nimis, P., Martin, S., and Mair, V., 2003, Mantle–crust interactions during Variscan subduction in the Eastern Alps (Nonsberg–Ulten zone): Geochronology and new petrological constraints: Earth and Planetary Science Letters, v. 210, p. 509–526, https://doi.org/10.1016/S0012-821X(03)00161-4.

Downloaded from http://pubs.geoscienceworld.org/gsa/geosphere/article-pdf/14/6/2311/4578874/2311.pdf
by guest

Tumiati, S., Godard, G., Martin, S., Klötzli, U., and Monticelli, D., 2007, Fluid-controlled crustal metasomatism within a high-pressure subducted mélange (Mt. Hochwart, Eastern Italian Alps): Lithos, v. 94, p. 148–167, https://doi.org/10.1016/j.lithos.2006.06.009.

Tumiati, S., Fumagalli, P., Tiraboschi, C., and Poli, S., 2013, An experimental study on COH-bearing peridotite up to 3.2 GPa and implications for crust-mantle recycling: Journal of Petrology, v. 54, p. 453–479, https://doi.org/10.1093/petrology/egs074.

Tumiati, S., Godard, G., Martin, S., Malaspina, N., and Poli, S., 2015, Ultra-oxidized rocks in subduction mélanges?: Decoupling between oxygen fugacity and oxygen availability in a Mn-rich metasomatic environment: Lithos, v. 226, p. 116–130, https://doi.org/10.1016/j.lithos.2014.12.008.

Tumiati, S., Tiraboschi, C., Sverjensky, D.A., Pettke, T., Recchia, S., Ulmer, P., Miozzi, F., and Poli, S., 2017, Silicate dissolution boosts the CO_2 concentrations in subduction fluids: Nature Communications, v. 8, article no. 616, https://doi.org/10.1038/s41467-017-00562-z.

Ulmer, P., and Trommsdorff, V., 1995, Serpentine Stability to Mantle Depths and Subduction-Related Magmatism: Science, v. 268, p. 858, https://doi.org/10.1126/science.268.5212.858.

Van Keken, P.E., Hacker, B.R., Syracuse, E.M., and Abers, G.A., 2011, Subduction factory: 4. Depth-dependent flux of H2O from subducting slabs worldwide: Journal of Geophysical Research. Solid Earth, v. 116, no. B1, https://doi.org/10.1029/2010JB007922.

van Roermund, H., Carswell, D., Drury, M.R., and Heijboer, T.C., 2002, Microdiamonds in a megacrystic garnet websterite pod from Bardane on the island of Fjørtoft, western Norway: Evidence for diamond formation in mantle rocks during: Geology, v. 30, no. 11, p. 959–962, https://doi.org/10.1130/0091-7613(2002)030<0959:MIAMGW>2.0.CO;2.

Vils, F., Pelletier, L., Kalt, A., Müntener, O., and Ludwig, T., 2008, The lithium, boron and beryllium content of serpentinized peridotites from ODP Leg 209 (Sites 1272A and 1274A): Implications for lithium and boron budgets of oceanic lithosphere: Geochimica et Cosmochimica Acta, v. 72, p. 5475–5504, https://doi.org/10.1016/j.gca.2008.08.005.

Vitale Brovarone, A., Alard, O., Beyssac, O., Martin, L., and Picatto, M., 2014, Lawsonite metasomatism and trace element recycling in subduction zones: Journal of Metamorphic Geology, v. 32, p. 489–514, https://doi.org/10.1111/jmg.12074.

Vrijmoed, J.C., Van Roermund, H.L.M., and Davies, G.R., 2006, Evidence for diamond-grade ultra-high pressure metamorphism and fluid interaction in the Svartberget Fe-Ti garnet peridotite-websterite body, Western Gneiss Region, Norway: Mineralogy and Petrology, v. 88, p. 381–405, https://doi.org/10.1007/s00710-006-0160-6.

Weiss, M., 1997, Clinohumites: A field and experimental study [Ph.D. thesis]: ETH-Zürich, 168 p.

Woodland, A.B., 2009, Ferric iron contents of clinopyroxene from cratonic mantle and partitioning behaviour with garnet: Lithos, v. 112, p. 1143–1149, https://doi.org/10.1016/j.lithos.2009.04.009.

Woodland, A.B., and Koch, M., 2003, Variation in oxygen fugacity with depth in the upper mantle beneath the Kaapvaal craton, Southern Africa: Earth and Planetary Science Letters, v. 214, p. 295–310, https://doi.org/10.1016/S0012-821X(03)00379-0.

Woodland, A.B., and Peltonen, P., 1999, Ferric iron contents of garnet and clinopyroxene and estimated oxygen fugacities of peridotite xenoliths from the Eastern Finland Kimberlite Province, *in* Nixon, P.S., ed., Proceedings of the 7th Kimberlite Conference: Cape Town, Red Roof Design, p. 904–911.

Woodland, A.B., Kornprobst, J., and Wood, B.J., 1992, Oxygen thermobarometry of orogenic lherzolite massifs: Journal of Petrology, v. 33, p. 203–230, https://doi.org/10.1093/petrology/33.1.203.

Woodland, A.B., Kornprobst, J., and Tabitc, A., 2006, Ferric iron in orogenic lherzolite massifs and controls of oxygen fugacity in the upper mantle: Lithos, v. 89, p. 222–241, https://doi.org/10.1016/j.lithos.2005.12.014.

Wunder, B., and Schreyer, W., 1997, Antigorite: High-pressure stability in the $MgO\text{-}SiO_2\text{–}H_2O$ (MSH) system: Lithos, v. 41, p. 213–227, https://doi.org/10.1016/S0024-4937(97)82013-0.

Xiao, Y., Niu, Y., Wang, K.L., Lee, D.C., and Iizuka, Y., 2016, Geochemical behaviours of chemical elements during subduction-zone metamorphism and geodynamic significance: International Geology Review, v. 58, p. 1253–1277, https://doi.org/10.1080/00206814.2016.1147987.

Yang, J., and Jahn, B.-M., 2000, Deep subduction of mantle-derived garnet peridotites from the Su-Lu UHP metamorphic terrane in China: Journal of Metamorphic Geology, v. 18, p. 167–180, https://doi.org/10.1046/j.1525-1314.2000.00249.x.

Zack, T., Kronz, A., Foley, S.F., and Rivers, T., 2002, Trace element abundances in rutiles from eclogites and associated garnet mica schists: Chemical Geology, v. 184, p. 97–122, https://doi.org/10.1016/S0009-2541(01)00357-6.

Zanchetta, S., Malaspina, N., Zanchi, A., Benciolini, L., Martin, S., Javadi, H., and Kouhpeyma, M., 2018, Contrasting subduction-exhumation paths in the blueschists of the Anarak Metamorphic Complex (Central Iran): Geological Magazine, v. 155, p. 316–334, https://doi.org/10.1017/S0016756817000218.

Zanetti, A., Mazzucchelli, M., Rivalenti, G., and Vannucci, R., 1999, The Finero phlogopite-peridotite massif: An example of subduction-related metasomatism: Contributions to Mineralogy and Petrology, v. 134, p. 107–122, https://doi.org/10.1007/s004100050472.

Zhang, Z., Xiao, Y., Hoefs, J., Xu, Z., and Liou, J.G., 2005, Petrogenesis of UHP metamorphic crustal and mantle rocks from the Chinese continental scientific drilling pre-pilot hole 1, Sulu belt, Eastern China: International Geology Review, v. 47, p. 1160–1177, https://doi.org/10.2747/0020-6814.47.11.1160.

Zheng, Y.-F., and Hermann, J., 2014, Geochemistry of continental subduction-zone fluids: Earth, Planets, and Space, v. 66, no. 1, p. 1–16, https://doi.org/10.1186/1880-5981-66-93.

Downloaded from http://pubs.geoscienceworld.org/gsa/geosphere/article-pdf/14/6/2311/4578874/2311.pdf
by guest